MASTERARBEIT / MASTER'S THESIS

Titel der Masterarbeit / Title of the Master 's Thesis

„Identification of Shipworms from the Northern Adriatic Sea“

verfasst von / submitted by

Charles Roque Figueiredo BSc

angestrebter akademischer Grad / in partial fulfilment of the requirements for the degree of

Master of Science (MSc)

Wien, 2023/ Vienna, 2023

Studienkennzahl lt. Studienblatt/ degree program code as it appears on the student record sheet:	UA 066 831
Studienrichtung lt. Studienblatt / degree programme as it appears on the student record sheet:	MA Zoology
Betreut von / Supervisor:	Univ.-Prof. Dr. Monika Bright

Acknowledgment

First, I want to thank Univ.-Prof. Dr. Monika Bright for supervising my thesis and making this all happening. Furthermore, I thank the PhD Students Salvador Espada-Hinojosa, Sebastian Valerio Aymerich and Teresa Maria Rosa Winter for sharing their knowledge in data analysis and laboratory work with me. I want to thank everybody from the Marine Benthic Ecology Group and, Functional and Evolutionary Ecology Department that helped me. Last but not least, I want to thank my family, friends and partner for supporting me along the journey of writing a master thesis.

Contents

Abstract

Shipworms are a highly adapted group of predominantly wood degrading bivalves. As wood consumers they present a big potential of destruction, while escaping most types of surveys. For my Master thesis I identified shipworms in the northern Adriatic Sea. At three different sites in Slovenia (Lera, Strunjan, Institute) wooden cubes were deployed from summer 2019 to summer 2022 with biannual sampling. The identification was based on morphology and sanger sequencing. I used the nuclear 18S rRNA barcode. For some shipworms, additional COI sequences were generated by Gäelle Berte. I identified four morphospecies. The final identification, using also the barcodes resulted in *Nototeredo norvagica, Teredo navalis* and the cryptic *Lyrodus mersinensis.* The morphospecies *Teredo bartschi* and *T. navalis* combined to *T. navalis.* The discrepancy could stem from my inexperience, but it also questions the recent morphological identification of *T. bartschi* in this region. The shipworm identification came with some hurdles but showed the importance of DNA barcodes. *Bankia carinata*, expected in the northern Adriatic Sea, was not found. In Strunjan and Institute our three species were present. In Lera, *N. norvagica* was not found. Temperature, salinity, and wood in the vicinity could not explain the presence/absence of the shipworms at our sites. Differences in sessile, filter feeding animal communities on the wood as well as differences in hydrogen sulphide produced during wood degradation and leaking from the wood may have an influence on shipworm distribution but this questions await future investigations.

Introduction

Shipworms (Teredinidae, Rafinesque, 1815) are a highly adapted group of predominantly wood degrading bivalves (Shipway et al., 2016; Shipway et al., 2019; Turner, 1966). They can be widely found in shallow waters across tropical and temperate seas as dominant wood consumers (Distel, 2003). Although until recently Teredinidae were thought to be restricted to shallow waters, they have been found in the deep sea (Velásquez & Shipway, 2018). The oldest fossil representative dates to the mid Cretaceous (Robin et al., 2018).

Shipworms are characterized by a long worm-like body with a reduced anterior shell and posterior pallets (Turner, 1971b). Their size can vary considerably. Shipworms can reach from a couple of centimetres up to 1.55 m in the giant shipworm *Kuphus polythalamius* (Linnaeus, 1767) (Distel et al., 2017; Turner, 1971a). Wood boring shipworms use their ridged shells to bore trough the substrate (Turner, 1971a). The wood is digested in the bacteria free gut with the help of imported enzymes. These are provided by endosymbiotic bacteria located in specialized cells in the gills (Connor et al., 2014). To what extent they depend on the substrate in comparison to filter feeding is unknown. Recent research on *Teredo navalis* suggests that shipworms gain most of their C and N intake from filter feeding (Johnson & Turner, 1971; Paalvast & Velde, 2011). The soft vulnerable body is shielded inside the substrate. Additionally, the tunnels are lined and strengthened with calcium carbonate that is secreted by the mantle (Treneman et al., 2018). Once settled most species are bound to the wooden substrate and keep contact to the outside only with the siphons (Distel et al., 2017; Turner, 1966). The incurrent siphon takes water in. The excurrent siphon releases water, waste and reproductive products. When disturbed or in unfavourable conditions, the tunnel is closed off by the pallets, allowing survival up to several weeks (Turner, 1971a). Shipworms show a variety of reproductive strategies. Johnson & Turner (1971) distinguished oviparous, and short term and long term larviparous species. The two latter breed their offspring in their gills to either the straight-hinged veliger or pediveliger stage (Johnson & Turner, 1971). Depending on the strategy the larvae stay from a few hours up to several weeks in open water (Turner, 1971a).

As one of the main taxa of wood degraders, shipworms play an important role in marine ecosystems (Johnson & Turner, 1971). They increase exposed wood surface and thereby allow other organisms to exploit this substrate. Also, by speeding up the degradation of wood, shipworms help keeping estuaries free from excess wood. Last but not least they present nutrients for other organisms in form of faecal matter and their bodies (Turner, 1971a).

While fulfilling an important role in nature, shipworms have been a pest for humans since the use of wood in the sea (Johnson & Turner, 1971). They infested harbours in 2000 B.C. and damaged warships influencing naval battles in ancient Mediterranean (Borojevic et al., 2010; Steinmayer & Turfa, 1996). Shipworms forced new technologies during the Dutch Shipworm Epidemic in the 1730s (Sundberg, 2015). "Teredo" even became an insult along the coast of the United States of America during the early 20th century (Nelson, 2018). Shipworms also earned the nickname “termites of the sea” due to often going undetected until the wood’s destruction (Turner, 1966). Nowadays, the impact of shipworms has decreased with the deployment of steel hulled ships, wood treatment and a better understanding of these creatures (Nelson, 2018). Shipworms still remain a threat causing over a billion dollars damage to wooden structures each year (Distel et al., 2011).

Scientifically, shipworms have been studied since the early 18th century. Sellius (1733) classified shipworms as molluscs. *Teredo* Linnaeus, 1758 was included in the 10th edition of the “Systema Naturae”, although not as a mollusc (Linnaeus, 1758). For two hundred years, the same species were often described by different people under different names, creating many synonyms (Turner, 1966). Turner (1966) tackled this problem, using among other data a lot of type material. This effort resulted in the reduction of almost three hundred previously described species to 66 species and either potential or real synonyms (Turner, 1966). A reason for this confusion was that for shipworms, in contrast to other bivalves, the shells are not usable for identification. Instead, the pallets are predominantly used to identify species (Turner, 1971b). The identification key of Turner (1971b) is, in combination with Turner (1966), used to this day for morphological identification of shipworms (Borges et al., 2022; Lee et al., 2019).

Still, shipworms remain a difficult group to identify (Turner, 1966). For example, pallets change their appearance during growth (Fuller et al., 1989). Ecological conditions can also lead to corroded, misshapen or worn-down pallets (Turner, 1966). The extraction of shipworms from wood is also challenging (Borges et al., 2012). This can often lead to incomplete samples with damaged pallets. The rise of molecular gene markers has become a useful addition for identification and shipworm research overall (Borges et al., 2012, 2022; Weigelt et al., 2016). It has led to the discovery of cryptogenic species and their descriptions (Borges & Merckelbach, 2018). These species are morphologically indistinguishable but differ genetically (Treneman et al., 2018). This shows the importance of DNA barcodes in shipworm identification. The most common barcodes are the nuclear small subunit 18S rRNA gene (18S) and the mitochondrial cytochrome c oxidase subunit 1 gene fragment (COI) (Borges et al., 2022; Borges & Merckelbach, 2018; Treneman et al., 2018). The 18S rRNA gene is sometimes used in combination with the nuclear 28S rRNA gene (28S) for phylogenetic relationship analysis (Lee et al., 2019; Shipway et al., 2019).

The Adriatic Sea measures 800 km in length and 200 km in width (Moranta et al., 2008). This semi-enclosed subbasin is part of the Mediterranean Sea and divided into a north, middle and south part. The shallow northern Adriatic Sea stretches from the Gulf of Venice to the Ancona-Zadar transect (Moranta et al., 2008). The northern and western coast of the northern Adriatic Sea is characterized by sandy beaches and surrounding flat land (Poulain et al., 2001). At the eastern coast are mainly cliffs interspersed with protected bays of sandy beaches. The east includes various islands, inlets, bays, and coves. The northern Adriatic Sea surface is heavily influenced by wind, heat, water fluxes, river run offs and the currents from the south (Poulain et al., 2001). Borges et al. (2014a) did a Europe wide shipworm survey. This combined old literature from 1900 to 2000 and field surveys from 2001-2011. They reported *Teredo navalis* Linnaeus, 1758, *Nototeredo norvagica* (Spengler, 1792), *Bankia carinata* (Gray, 1827) and *Lyrodus pedicellatus* (Quatrefages, 1849) in the northern Adriatic Sea. At that time an Atlantic and a Mediterranean form was distinguished in *L. pedicellatus* (Borges et al., 2012; Borges et al., 2014a). The latter has been described recently as the cryptic species *Lyrodus mersinensis* Borges & Merckelbach, 2018. The Mediterranean Sea accommodates also *Teredora malleolus* (Turton, 1822), *Teredo bartschi*

Clapp, 1923 and *Teredothyra dominicensis* (Bartsch, 1921). According to Borges et al. (2014a) the latter two are alien to the Mediterranean. In 2014, the first established population of *T. bartschi* was documented in Mersin, Turkey (Borges et al., 2014b). Recently, it's occurrence in the Lagoon of Venice was recorded (Tagliapietra et al., 2021). Shipway et al. (2014) revealed the establishment of *T. dominicensis,* a Caribbean teredinid, in the eastern Mediterranean. The National Center for Biotechnology information (NCBI) database (GenBank) (Sayers et al., 2022) the barcodes 18S, 28S and COI for *Bankia carinata, L. pedicellatus, N. norvagica* and *T. navalis*. *L. mersinensis* is represented by COI and 18S. The GenBank database holds two complete mitochondrial genomes for *T. bartschi*, but no nuclear barcodes. Some COI barcodes of *T. bartschi* exist on the Barcode of Life Data System (BOLD), but are not publicly available (Ratnasingham & Hebert, 2007). Invasive species are often detected after establishment and causing sufficient damage**.** This is due to the difficulties in their detection during the early colonisation phase (Kamburska et al., 2013)**.** This is especially true for shipworms, as they elude most types of surveys (Borges et al., 2014a). Combined with the destructive potential of shipworms it is very important to target these animals directly.

For my Master thesis I identified shipworms in the northern Adriatic Sea. Wooden cubes were deployed at three different sites along the Slovenian coast. The first site is in a manmade canal, serving to fill the salt plans and control the seawater flow in the Sečovlje Salina Nature Park (Lera). The canal ground is muddy and rich in sea grass and sea anemones. The deployment is attached to a wooden bridge at 2.5 m depth. The second site is located in the Landscape Park Strunjan (Strunjan). It is in an inter- to subtidal mud flat at 1.5 m depth, next to a small harbour at the entrance of the Laguna stjuža. This site is also characterised by muddy sediment with seagrass and sea anemones. The third site is in front of a manmade stony beach in Piran, in a wave exposed area covered by muddy sand at about 3.5 m depth. It is next to the Marine Biology Station Piran. Deployment of the wooden cubes was in summer 2019. Sampling of 3 cubes per site for each season was done in winter 2020, summer 2021, and winter 2021. Data for ecological comparisons were taken from the entire experiment from winter 2020 until summer 2022. The shipworms were identified based on morphology and molecular data. I used for this study the widely applied nuclear 18S rRNA

sequences as molecular markers. In bivalve species 18S rRNA sequences were shown to have low interspecific distances and no intraspecific variability (Espińeira et al., 2009). Borges et al. (2012) described the same pattern in shipworms. For some samples the COI sequences were additionally generated as a second barcode by the intern Gäelle Berte.

This thesis aimed to study the presence of Teredinidae species among different habitats at the Slovenian coast.

1. Based on Borges et al. (2014a) and Borges & Merckelbach (2018) I hypothesize to find the species *Bankia carinata, Nototeredo norvagica, Teredo navalis* and the recently described *Lyrodus mersinensis* (formerly *L. pedicellatus* Mediterranean population).
2. Additionally, I hypothesize to encounter *Teredo bartschi.* This species has colonized recently in the lagoon of Venice in the northern Adriatic Sea and thousands of ships arrive at Slovenia coast 90 km away from Venice, each year (Kos, 2021; Tagliapietra et al., 2021).
3. Further, I hypothesise differences in species presence and time of colonization at the three studied sites. At Lera and Strunjan colonization may be easier with source populations on plenty of wood present, while at the Institute colonization may be more difficult and/or later due to the lack of source populations as no wood is present nearby.

Material and Methods

Sample collection and fixation

The shipworms were collected from deployed wood at three different sites along the Slovenian coast (Figure 1).

Figure 1: Location of our sampling sites. Top left: Overall map from the Mediterranean with Piran marked as a white dot. Top right: Map of the Slovenian coast with our sites Lera (blue), Strunjan (yellow) and Institute (red). Bottom: Close up maps for each site (Map source: Google Earth).

The first site (Lera) is situated in an estuarine canal next to salt pans in the Sečovlje Salina Nature Park (Coordinates: 45°29'41.1"N 13°35'45.1"E). The sampling structure, termed Biological Recruitment Grid, short BORG, is attached

to a wooden bridge at 2.5 m depth. The canal ground is made of muddy sediment. It is abundant on sea grass and sea anemones. The second site (Strunjan) is in the entrance of the Laguna stjuža in the Landscape Park Strunjan (Coordinates: 45°31'41.5"N 13°36'17.4"E). Strunjan is located in an inter- to subtidal mud flat, next to a small harbour. This site has also muddy sediment with seagrass and sea anemones. This site has a lot of wood nearby. In 1.5 m depth, Strunjan is the shallowest site among the three. The third site (Institute) is in front of a stony beach next to the Marine Biology Station Piran (MBS) (Coordinates: 45°31'02.6"N 13°34'04.3"E). This site is characterised by muddy sand on the seafloor and exposure to waves. It has little structures around and is the most exposed site out of the three. With 3.5 m depth it is our deepest site. There is no wood in direct vicinity. With the beach nearby, there is human activity in the proximity.

In summer 2019, one BORG was deployed at each site. Each BORG consisted of an iron frame with 30 wooden and 10 plastic cubes (Figure 2). The cubes were attached with cable ties at three different levels, the bottom, middle or top. All levels were submerged in water all year round.

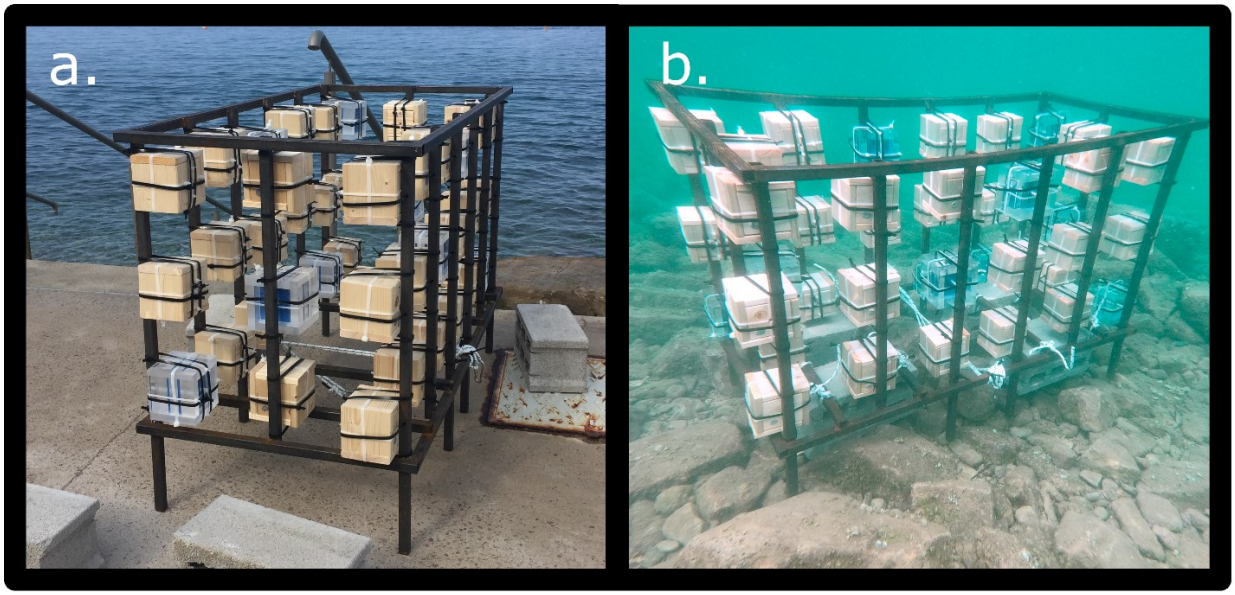

Figure 2: BORG (Biological Recruitment Grid) before (a.) and after (b.) deployment at the Institute in summer 2019 (©Bright Lab).

The cubes were formed of three centre and six outer plates (Figure 3). Each side had a thickness ranging from 0.5 cm to 2 cm. Each cube had a hole of 1 cm diameter going through the centre to allow envelopment with cable ties. Next to it was a smaller hole, reaching the middle of the cube. This one was sealed to

measure the inside cube conditions in the lab. The wooden cubes were made from dried, untreated pinewood. Each measured 11.2 cm*11.2 cm*12 cm. The plastic cubes were made from inert acrylic glass and measured 13 cm*13 cm*13 cm.

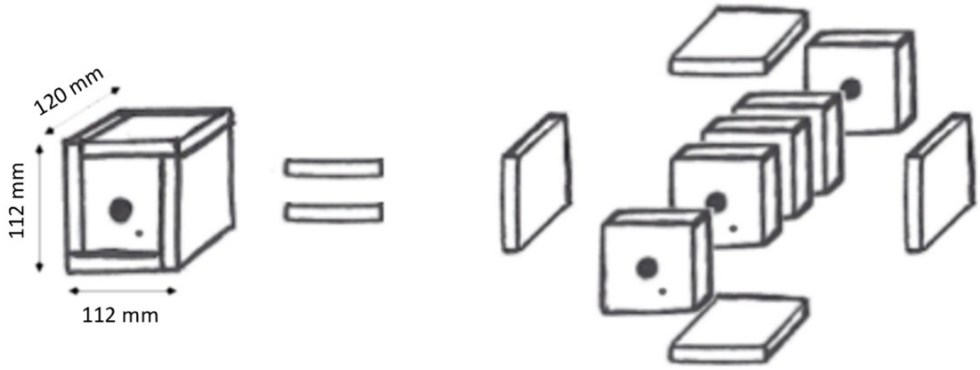

Figure 3: Wooden cube scheme (112m*112mm*120mm). It has a bigger hole of 1cm diameter running through the centre for attachment. The smaller hole is sealed and does not go through to the other side. The cube is made of 5 centre parts (with holes) and 4 sides.

Sampling occurred in Winter 2020, Summer 2020 and Winter 2021. Each research stay, one wooden cube per level per site was collected. In addition, one plastic cube per site with a random level was taken. The plastic cubes were not relevant for this study as shipworms did not settle on this substrate. Depending on how many cubes were retrieved together, we visited the sites multiple times during one season. At each cube retrieval we measured the oxygen (O_2), temperature (T°), pH and salinity from the water at the surface and next to the BORGs. The water was taken in cups with lids and measured on site during cube sampling. The T° and O_2 were measured with the Fibox 4 (PreSens, Germany). The WTW Multi 340i (Wissenschaftlich-Technische Werkstätten, Germany) was used to measure the salinity and pH. The cubes were brought back to the lab in buckets with lids. At the lab the sealed hole was opened. We measured the T°, O_2, pH and salinity from the cube inside by inserting the dipping oxygen probe. We used the same instruments as before. The measurements from the inside of the wood were taken for comparisons of shipworm species presence in time and at sites. Afterwards the cubes were taken apart. Each side and the five centre plates were photographed from both sides. These pictures were made with the Olympus Tough TG-6 in a big bucket of saltwater (Figure 4). The outside plates were all marked with the letters A-F. E and F represented always the two outside plates from the centre. After the

photoshoot, we placed all plates in our saltwater flow through systems. The system consisted of plastic containers with two hoses. Each container had a hose where saltwater was flowing in. The second hose was attached to a hole near the top of the tub. This prevented overflowing without washing out anything falling of the plates. Each cube got placed separately in a flow-through container, not to mix up organisms. The flow through system was used to keep the organisms on the plates alive.

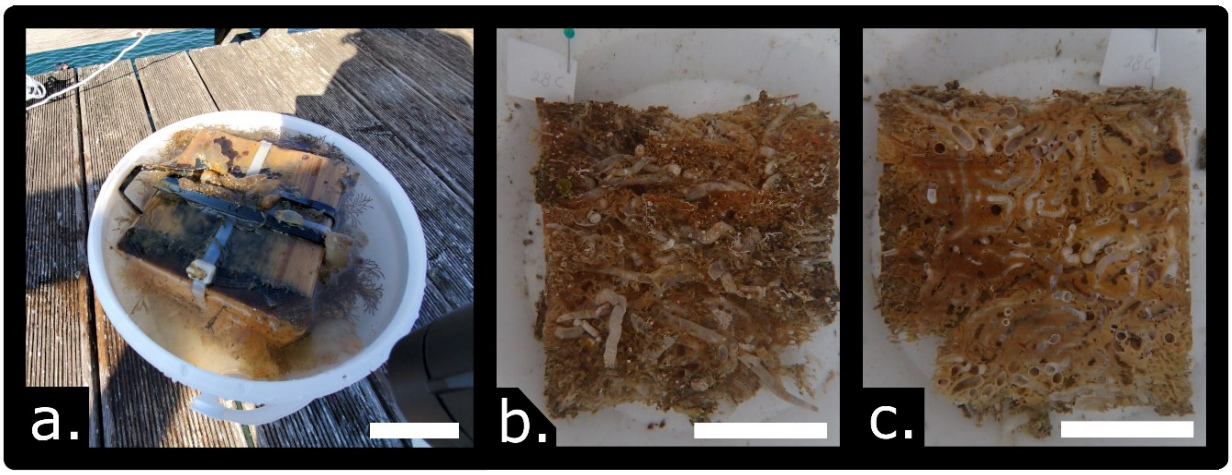

Figure 4: Wooden cube in bucket on site, collected Winter 2020 (a.). Outside (b.) and inside (c.) view of side plate C, cube 28, with abundant shipworm tunnels (scalebar (white) = 5cm; camera: Olympus Tough TG-6) (©Bright Lab).

Shipworms were collected from all plates, centre and sides. I examined the plates one after the other with the MOTIC SMZ-168 Stereo Zoom microscope. The extraction was done with a pair of teasing needles and tweezer. To break the wood, I used sturdy forceps. A glass dropping pipette was used to keep the plates clean while working. I searched for protruding siphons. Once found, I tried to free the area around the aperture from wood and lay more of the calcareous tunnel free. With this I tried to break the tube further down to be able to grab under the pallets to keep them intact while pulling the shipworm out. However, it is difficult to break the tube without damaging the soft body inside. If disturbed too much they retreated further inside their tunnel and close it off with the pallets. This approach was used for the side plates and the two outside centre plates. These were needed for purposes outside this study and needed to stay intact. The inner centre plates were not needed further, which allowed another approach. Here I looked rather for tunnels than for protruding siphons. I poked into each tunnel to see if a shipworm was inside. In case of a shipworm, I started to take off the wood and lay

most of the tunnel free. Then I broke it off along the whole animal if possible. This was not always achieved as the tunnels can turn and twist along the way. Despite the hind part being the most valuable for identification, I aimed for the head in this search. The hard structure gives a good surface to grab the animal and pull it out. The soft body was not suitable for this and broke easily. The pallets are easy to damage. Therefore, the head was most suited for this. This resulted in a lot of intact animal extractions. After following a couple of tunnels and poking into the others, most plates were quite dismantled. After sampling, the shipworms were photographed with a Canon EOS 550D mounted to a BMS Stereo Trino Zoom microscope. This setup was placed on a BMS Boom stand. These pictures were used for the morphological identification later. After the photoshoot the shipworms were stored in 100% ethanol and kept in the fridge at 4°C.

Morphology

The morphological identification was based on the identification key for marine wood-boring molluscs (Turner, 1971b) and illustrations in Turner (1966). The pictures from Borges et al. (2014a) and Tagliapietra et al. (2021) were used as reference too. The shipworms were identified based on the pallets and siphons (Figure 5). These are located at the posterior end. Siphons are divided in the incurrent and excurrent siphon. The incurrent siphon is used for water intake. Waste and reproductive products are released from the excurrent siphon. Pallets are the most important structure for identification. They consist of a blade and a stalk. The blade is made of a hard calcareous base and a more fragile periostracum. In Teredinidae, the periostracum varies from a thin layer surrounding the base to being a separate structure on top. The shape of the calcareous base and the periostracum are the main characters. The colour of the periostracum also plays a role. In case of missing or damaged pallets our shipworms were identified on family or genus level.

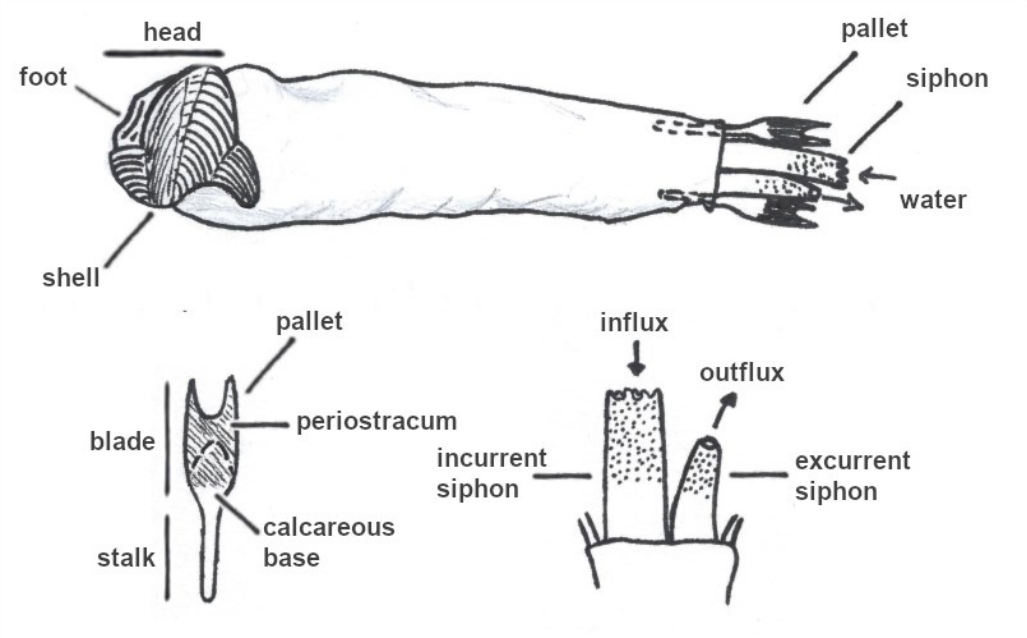

Figure 5: Shipworm scheme with a whole animal on top, a pallet in bottom left and the siphons in bottom right. The scheme is drawn after the morphology of *Lyrodus pedicellatus/mersinensis*.

DNA extraction

The DNA extraction was done using the DNeasy kit (QIAGEN, Valencia, CA) according to "The Protocol: Purification of Total DNA from Animal Tissues (Spin-Column Protocol)". Before first use, we diluted the 242 ml wash buffer concentrate (Buffer AW1) and the 324 ml wash buffer concentrate (Buffer AW2). For this we added 100% ethanol as indicated on the bottles to obtain working solutions. As preparation for the extraction, I preheated the thermomixer to 56°C. I disinfected petri dishes (1 per sample), forceps and 1.5 ml microcentrifuge tubes (2 per samples) under UV for 30 min. These were used in addition to sterile razor blades to prepare the samples for lysis. I cut off 1-2 mm from the posterior half of the animals, avoiding most organs and leaving the pallets and siphons intact. These tissues were then cut smaller with razor blades and placed in the UV treated 1.5 ml microcentrifuge tubes. Once cut, I added 180 µl of the tissue lysis buffer (Buffer ATL) and 20 µl proteinase K to the tubes. These were then vortexed and put in the preheated thermomixer at 56°C for lysis. Tissue parts that were outside of the liquid after mixing were pushed in the liquid with sterile pipetting tips. As lysis time varies depending on the tissue, the samples were lysed overnight for convenience. After lysis the samples were vortexed for 15 s. Then 200 µl of the lysis buffer (Buffer AL) was added and the samples vortexed again. Immediately after, 200 µl of 100% ethanol was added, and the samples mixed again. In case of the

formation of white precipitate, we vortexed further to help it dissolve. Regardless of state of dissolution, I proceeded with the protocol since according to manufacturer's instruction, the remaining precipitate did not affect the extraction. The samples were then pipetted into DNeasy Mini spin columns, which were placed in 2 ml collection tubes. The tubes were then centrifuged at 8000 rpm (6000 x g) for 1min. The DNeasy Mini spin columns were placed in new 2 ml collection tubes. The flow-through and old collection tubes were discarded. I added 500 µl Buffer AW1 to the columns in the new tubes and centrifuged again at 8000rpm (6000 x g) for 1 min. The flow-through and collection tubes were discarded after placing the DNeasy Mini spin columns again in new 2 ml collection tubes. 500 µl Buffer AW2 was added and samples were centrifuged at 14000 rpm (20000 x g) for 3 min drying the DNeasy membrane. The flow-through and collection tubes were discarded. The DNeasy Mini spin columns were removed carefully not touching the flowthrough. The columns were placed in the second UV treated 2 ml microcentrifuge tubes. I added 100 µl elution buffer (Buffer AE) directly on the membrane and incubated the tubes for 1min. These were then centrifuged at 8000 rpm (6000 x g) for 1min for elution. Any kind of troubleshooting or important information on the procedure are addressed in the complete DNeasy kit (QIAGEN, Valencia, CA) protocol. According to the material safety data sheet (MSDS) Buffer ATL contained 1-5% sodium dodecyl sulphate, Buffer AL 20-50% guanidinium thiocyanate and Buffer AW1 10-40% guanidine hydrochloride. The MSDS did not specify any components of Buffer AW2 and AE, as they did not contain any substances in concentration considered hazardous to health (https://www.abpbio.com).

Polymerase chain reaction (PCR) and Sanger sequencing

Almost the total length of the 18S rRNA gene was amplified with the primers 82 Forward (5'GAA ACT GCG AAT GGC TC) (Elwood et al., 1985) and Medlin B Reverse (5'TGA TCC TTC TGC AGG TTC ACC) (Medlin et al., 1988). The PCR was performed in 50 µl reactions. These contained 34.3 µl UltraPure DNase/RNase-Free distilled water (Thermofisher), 5 µl Puffer (Fermentas + KCl, 2 mM), 5 µl dNTP (2mM), 4 µl MgCl (25mM), 0.5 µl of each primer, 0.5 µl Bovine Serum Albumin (invit 1mg/ml), 0,2 µl Taq polymerase (5U/µl) and 1 µl of extracted

sample DNA. We used the following PCR program: First DNA denaturation was one cycle at 95°C for 3 min. Then followed 30 cycles of denaturation at 95°C for 30 s, annealing at 60°C for 30 s and extension at 72°C for 90s. The final extension was at 72°C for 10 min. The PCR product was then cooled to 4°C and stored at -80°C. The PCR product was visualized in a gel electrophorese as quality control, before being sequenced. The gel was loaded with 2.5 µl PCR product or 2 µl Gene-Rule 1kb DNA Ladder (Thermo Scientific) and 2 µl Loading Dye (1.25x). The Loading Dye 1.25x working solution was diluted from 6x DNA Loading Dye stock solution (Thermo Scientific) beforehand. The samples, plus a positive control, went through a Gel electrophoresis of 90 V for 50 min in a 1% agarose gel. The DNA was stained in a SYBR™ Gold bath for 35 min. Afterwards the gel was visualised in a Bio-Rad Universal Hood II Gel Doc System under TransUV. Purification & Sanger sequencing of the samples was done with the Economy Run Plus (Plate) from Microsynth Austria GmbH.

The mitochondrial cytochrome c oxidase subunit I gene (COI) was sequenced for a selection of the shipworm DNA extracts by Gäelle Berte as part of an internship. The COI sequences were amplified with the universal forward primer LCO 1490 (GGTCAACAAATCATAAAGATATTGG) and the reverse primer HCO 2198 (AAACTTCAGGGTGACCAAAAAATCA) (Folmer et al., 1994). The same DNA extracts were used or if needed the DNA was extracted following the same protocol as above. The PCR procedure started the same, except with a different PCR program: The first DNA denaturation was on cycle at 95°C for 1 min. This was followed by 35 cycles of 95°C for 1 min, 40°C for 1 min and 72°C for 1:30 min. The final extension was 5 min at 72°C. The COI amplification did not work for some shipworms, later identified as *Teredo navalis*. Here the *T. navalis* specific forward primer Ter_fw II4 (GTTTCTGGTTAATGCCTAGATC) and reverse primer Ter_rev I4 (GCTCTGGATACGACAATCCCAG) were used instead (Weigelt et al., 2016). The procedure was the same but used a different PCR program: One cycle at 92°C for 1min. This was followed by 35 cycles of 1min at 95°C, 1min at 40°C and 1:30 min at 72°C. The final extension was 5 min at 72°C.

Data analysis

The Sanger sequencing resulted in a forward (F) and reverse (R) sequence for each sample. For the following analysis I used Geneious Prime® 2021.1.1 (www.geneious.com). These steps were done based on Exercise 2a/b from the "Assembling Chromatograms" tutorial of Geneious Prime®. First, the chromatograms of our sequences were imported into the program. I annotated the poor-quality ends of our samples. This was done under **Annotate and Predict->Trim Ends-> Annotate new trimmed regions.** The error probability limit was set to 0.01, the default setting. The trimmed/annotated regions were ignored in the assemblage of the F and R sequences. Next, I checked for heterozygotes according to the tutorial. This was done under **Annotate and Predict->Find Heterozygotes. Peak similarity** was set at 50%. **Search Trimmed regions** was disabled and **Annotate** was chosen. The next step was to assemble the F and R sequences. All F sequences were selected and got assigned their direction with **Sequence-> Set Read Direction-> Forward.** This was not done for the R sequences as it happens automatically during the assembling. All F and R sequences were selected and assembled with **Align/Assemble->DeNovo Assemblage**. In **Assemble by**, I selected the first part of the name. As this was the sample ID, the F and R of each sample were put together. The settings **Highest Sensitivity/Slow**, **Save assembly report**, **Save list of unused reads**, **Save in sub-folder**, **Save contigs** and **Use of existing trim regions** were checked. The last one ensures that the annotated ends are excluded in the assemblage. With this the F and R sequences were aligned and assembled. If a F and/or R sequence were not usable, they were shown in the unused read list. These samples were if possible sequenced again or left out from further analysis. In the next steps I checked the assembled sequences and extracted the consensus sequence. In Geneious Prime®, the assemblages are shown with the chromatograms of the F and reverse complementary R sequences. **Display->Consensus->Highest Quality** was chosen. This showed the consensus sequence, based on the highest signal strength, on top of the chromatograms. To add the original base numbering for the two sequences, **Advanced->Base numbers->All Sequences** was selected. I also enabled **Coverage** and **Identity** under **Graphs**. **Coverage** visualized on how many sequences the consensus was based for each base. **Identity** showed if the two sequences agreed or disagreed

for each base. With all this enabled, I checked the assemblages visually. In case of disagreement between the sequences the following was done. If base signals in the chromatogram were of similar strength, I used the according letter from the International Union of Pure and Applied Chemistry (IUPAC) code for ambiguities (Cornish-Bowden, 1985). In case of a base signal being way weaker in contrast to the other at the same position, the stronger base signal was chosen for the consensus sequence. The latter case was usually already changed by Geneious Prime®. Despite automatic correction, these positions were checked on visually. After checking the chromatograms, I extracted the consensus sequence for each sequence. These were then used for further analysis. The consensus sequences were compared to the NCBI database (GenBank) with BLAST (Altschul et al., 1990). With this I checked if I amplified shipworms sequences and no endosymbiont or contaminant instead. The best hits from the BLAST search were added as reference to further analyses (Tables 1-2).

Table 1: Species name, location, accession number and source of the 18S sequences from GenBank used in this study.

Species name	**Collection site**	**Accession number**	**Source**
Bankia carinata	no data	AF120564	Giribet & Wheeler 2005
Bankia carinata	Lac Bay, Bonaire, Netherlands Antilles	JF899203	Distel et al. 2011
Lyrodus pedicellatus	Portsmouth, United Kingdom (UK)	AM774540	Taylor et al. 2007
Lyrodus pedicellatus	Banana River, Florida, mangrove wood	JF899211	Distel et al. 2011
Lyrodus pedicellatus	Brittany, France 47°36'08.8"N, 2°51'32.7"W	KU201120	Weigelt et al. 2016
Lyrodus pedicellatus	Brittany, France 47°36'08.8"N, 2°51'32.7"W	KU201121	Weigelt et al. 2016
Lyrodus pedicellatus	Brittany, France 47°36'08.8"N, 2°51'32.7"W	KU201122	Weigelt et al. 2016
Lyrodus pedicellatus	Mersin, Turkey, Mediterranean Sea 36°48'20.1"N, 34°39'22.3"E	KU201123	Weigelt et al. 2016
Nototeredo norvagica	Mersin, Turkey, Mediterranean Sea 36°48'20.1"N, 34°39'22.3"E	KU201117	Weigelt et al. 2016
Nototeredo norvagica	Mersin, Turkey, Mediterranean Sea 36°48'20.1"N, 34°39'22.3"E	KU201118	Weigelt et al. 2016
Nototeredo norvagica	Mersin, Turkey, Mediterranean Sea 36°48'20.1"N, 34°39'22.3"E	KU201119	Weigelt et al. 2016

Teredo navalis	Belfast, Maine, United States of America (USA)	JF899222	Distel et al. 2011
Teredo navalis	Nienhagen, Baltic Sea, Germany, 54°9'54.86"N,11°57'7.01"E	KU201114	Weigelt et al. 2016
Teredo navalis	North America East Coast 44°25'46.1"N,69°00'20.3"W	KU201115	Weigelt et al. 2016
Teredo navalis	Mersin, Turkey, Mediterranean Sea 36°48'20.1"N, 34°39'22.3"E	KU201116	Weigelt et al. 2016
Martesia striata	Florida, USA	KX713311	Combosch et al. 2017

Table 2: Species name, location, accession number and source of the COI sequences from GenBank shown in this study.

Species name	**Collection site**	**Accession number**	**Source**
Teredo bartschi	Coos Bay, Oregon, USA 43°19'32.9"N, 124°12'22.5"W	NC063766.1	Li et al., 2022
Teredo navalis	Nienhagen, Baltic Sea, Germany, 54°9'54.86"N,11°57'7.01"E	KU201140.1	Weigelt et al., 2016
Teredo navalis	Wangerooge, North Sea, Germany 53°46'32.6"N,7°52'04.2"E	MF071124.1	Weigelt et al., 2017
Nototeredo norvagica	Mersin, Turkey, Mediterranean Sea 36°46'48.0"N 34°39'00.0"E	KC157926.1	Borges et al., 2012
Lyrodus pedicellatus	Toulindac, Brittany, France 45°21'00.0"N 2°31'12.0"W	KC157917.1	Borges et al., 2012
Lyrodus mersinensis	Mersin, Turkey, Mediterranean Sea 36°19'48.0"N 34°21'00.0"E	KC157916.1	Borges et al., 2012
Lyrodus mersinensis	Mersin, Turkey, Mediterranean Sea 36°19'48.0"N 34°21'00.0"E	KC157939.1	Borges et al., 2012
Pecten jacobaeus	Turkey	KC789373.1	Keskin, un-published

The phylogenetic trees were made in SeaView Version 5.0.4 (Gouy et al., 2010). First our and the GenBank sequences were imported. Due to very short sequences, the samples 6295 and 6562 were excluded at this point from the data analysis. The remaining sequences were aligned using muscle alignment (Edgar, 2004). These were then trimmed at both ends. The new first and last position correspond to 90% or more coverage by all sequences. This was done to make our sequences more comparable.

Based on obtained sequences I made a Maximum Likelihood (Guindon et al., 2010) and Maximum Parsimony phylogenetic tree (Felsenstein, 2013) with 1602

bp. I used the default settings for both trees in Seaview with the addition of 100 Bootstrap replicates (Figure 6). These trees were saved under the Newick Tree file format (.nwk) (Archie et al., 1986) and exported from Seaview. For more visualization and editing, I used MEGA11: Molecular Evolutionary Genetics Analysis version 11 (Tamura et al., 2021). The Maximum Likelihood tree using the COI sequences was made in a similar fashion by Gäelle Berte.

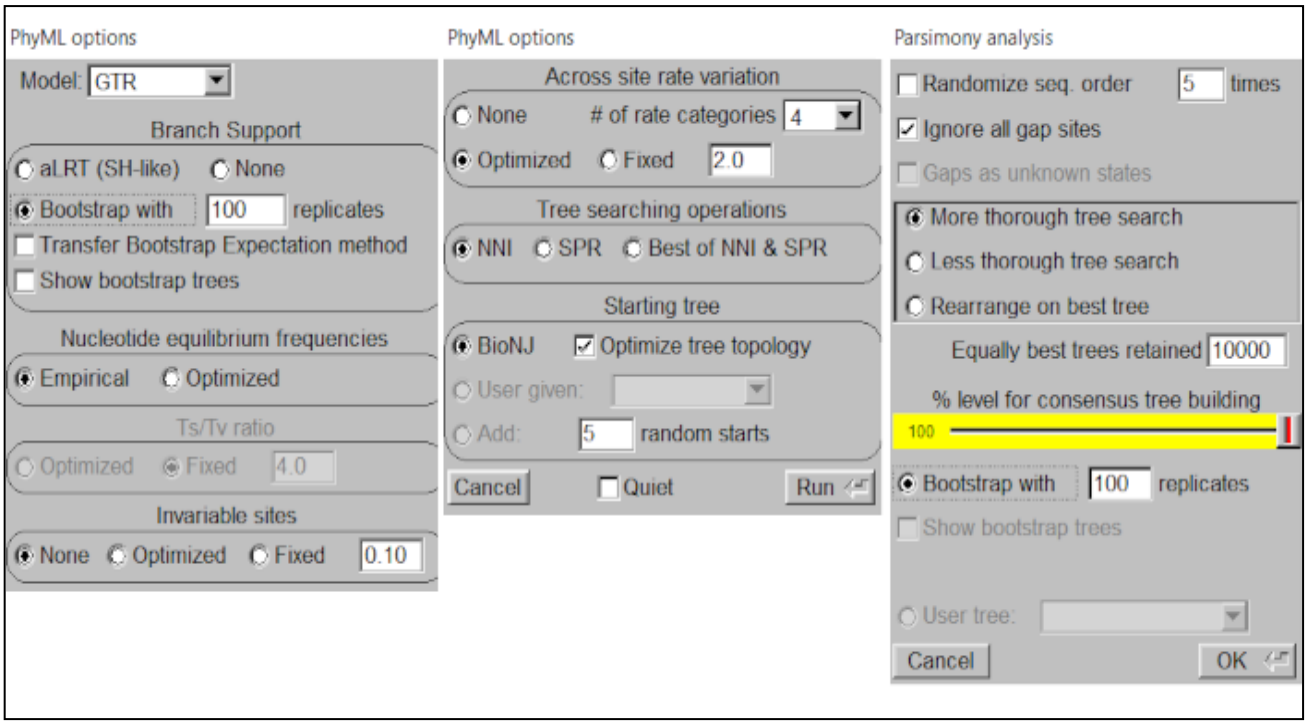

Figure 6: Settings for the Maximum Likelihood (here: PhyML) and Maximum Parsimony phylogenetic trees used in SeaView Version 5.0.4.

The Pairwise distances were calculated in RStudio Version 2021.09.1.372 (R Core Team, 2013) (Figure 7). We used the packages “ape” version 5.6.1 (Paradis & Schliep, 2019) and “seqinr” version 4.2.8 (Charif et al., 2021). Per preference, the distances were converted into similarity in %. The similarities between all samples were then exported from RStudio as an overall table into Microsoft® Excel® Version 2207 (Microsoft Corporation, 2018). In Excel®, I used this table to calculate the inter- and intraspecific similarities.

The spearman correlation was done in RStudio Version 2021.09.1.372 (R Core Team, 2013) with the packages “readxl” version 1.4.1(Wickham & Bryan, 2022), “tidyverse” version 1.3.2 (Wickham et al., 2019), “ape” 5.6.1 (Paradis & Schliep, 2019) and “seqinr” version 4.2.8 (Charif et al., 2021), “writexl” version 1.4.2 (Ooms, 2023) and “Hmisc” version 5.0-1 (Harrel Jr., 2023). The spearman matrix

was visualized with a script from Paul van der Laken (2020). The plot was made with the package “ggplot2” version 3.4.0 (Wickham et al., 2016) from the “tidyverse” package. Final visualisations were made in GIMP 2.10.32 and Excel®.

Shipworm pictures taken with the Canon EOS 550D, were saved as RAW format to keep high picture quality. To view RAW format pictures, I used the Digital Photo Professional 4 version 4.15.0.0. Picture editing was done in GIMP 2.10.32 (Revision 1) and Microsoft® PowerPoint® version 2207 (Microsoft Corporation, 2018).

```
setwd("~/withCharly_Mar2022")

library(ape)

library(seqinr)


###Distance calculations

shipworms<-read.dna("Shipworm_18s_original_aligned_sorted.fasta","f")

round(100-dist.dna(shipworms,model="raw")*100,2)

#round(100-dist.dna(shipworms[c(1:47),],model="raw")*100,1)

#round(100-dist.dna(shipworms,model="raw")*100,1)

round(100-dist.dna(shipworms,model="raw",pairwise.deletion=TRUE)*100,2)


##Exporting Distances to exel

object<-round(100-dist.dna(shipworms,model="raw",pairwise.deletion=TRUE)*100,2) # define our distance as object

class(object)

object2<-as.matrix(object)

head(as.matrix(object))


Rnew<-object2

Rnew[upper.tri(Rnew, diag = TRUE)] <- ""

distances_all <- as.data.frame(Rnew)
```

Figure 7: Code for Pairwise distance/similarity calculations in % and export to Microsoft® Excel® used in R Studio.

Results

Morphological identification

I studied the morphology of 56 samples. 28 samples were identified to species level, and 12 samples to genus level. 16 samples were identified as Teredinidae based on pictures of body parts like siphons, heads/shells or highly damaged pallets. The analysis resulted in four morphospecies, *Lyrodus cf. mersinensis* (5 specimens), *Nototeredo norvagica* (19 specimens), *Teredo bartschi* (3 specimens), and *Teredo navalis* (1 specimen).

One of them was the cryptic species *Lyrodus mersinensis.* It was formerly described as the Mediterranean variant of *Lyrodus pedicellatus* (Borges et al., 2012; Borges et al., 2014a). *Lyrodus mersinensis* is morphologically identical to *Lyrodus pedicellatus* and can only be distinguished from other *L. pedicellatus* by differences in the COI gene and a single position in the 18S rRNA (Borges & Merckelbach, 2018). Based on the geographical data, I used the morphological description of *L. pedicellatus* from Turner (1971b) and tentatively identified five specimens as *Lyrodus cf. mersinensis.* Their pallets were not segmented. The calcareous base constituted of a single piece with a conical distal end. The periostracal cap covered the upper part of the calcareous base and went beyond distally. The periostracal cap was roughly straight sided and often extended as lateral horns (Figure 8, d). The periostracum varied from light brown to nearly black. The distal margin of the pallets was slightly concave to U-shaped (Figure 8). Ten samples had a damaged periostracum, making it not possible to differentiate between several species of the genus *Lyrodus.* These were identified as *Lyrodus* sp..

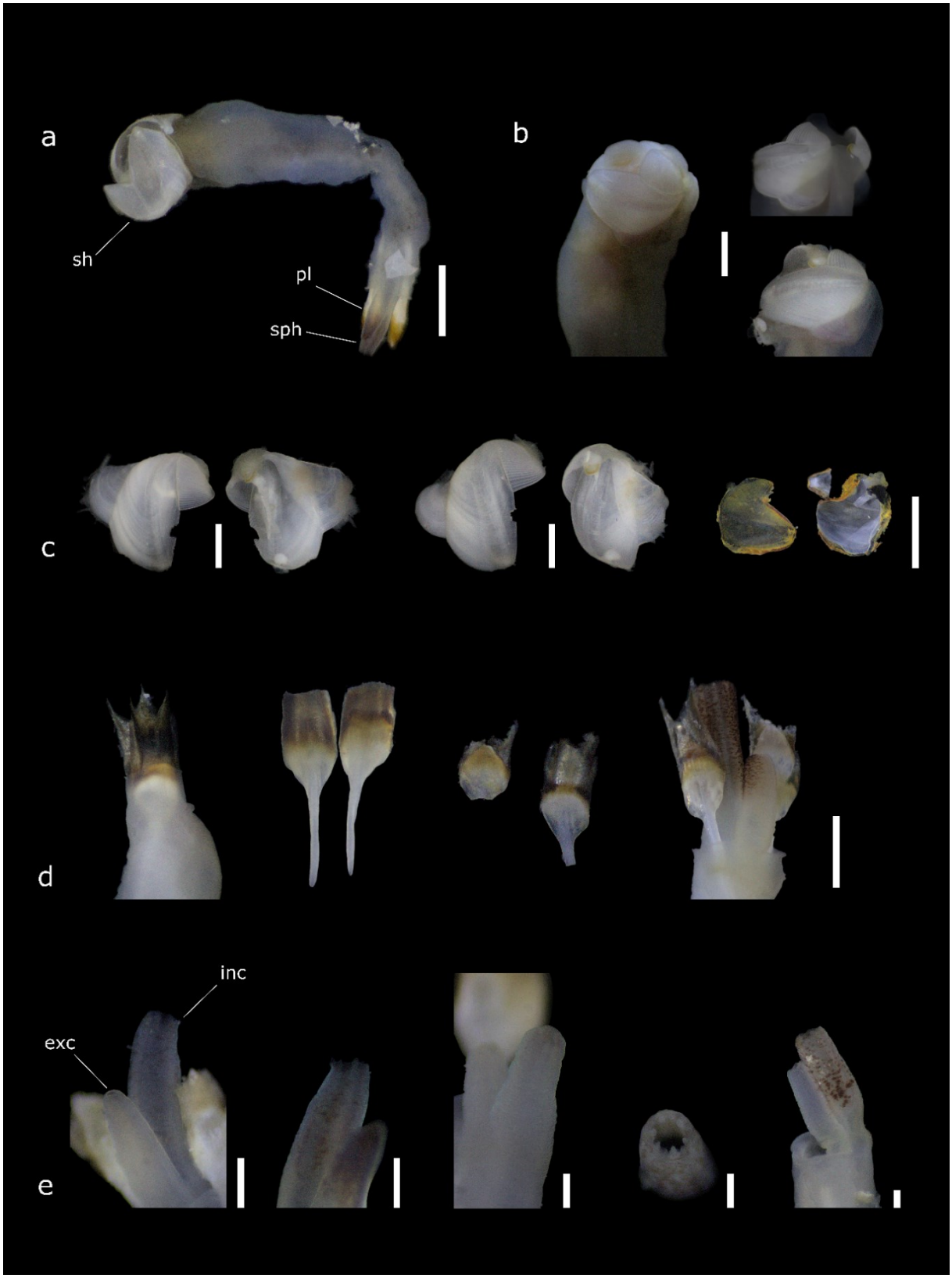

Figure 8: Micrographs of *Lyrodus cf. mersinensis*. a) whole individual (sample 6281) with shell (sh), pallets (pl) and siphons (sph); b) heads (samples: left 5212; right top 6385; right bottom 6405), c) shells (samples left to right: 6423; 6426; 6258), d) pallets (samples left to right: 6424; 5277; 6405; 5265), e) excurrent (exc) and incurrent (inc) siphons (samples left to right: 6255; 6281; 6293; 6429; 6405). Scale bar (a-d) = 2mm, scale bar (e) = 0.5mm.

The second morphologically identified species was *Nototeredo norvagica.* I referred to the identification key of (Turner, 1971b), but did not use the confusing siphon description for its identification. The same approach was applied in Borges et al. (2012). I identified 19 specimens as *N. norvagica.* Their pallets were segmented. The segments were closely packed, fused, indistinct and radiated from the stalk. The stalk reached almost blade length. The blade was shaped like a paddle. The pallets had a small thumbnail depression at the distal end. It was broadest distally and became narrower towards the proximal end. The yellowish periostracum was faintly visible. Turner (1971b) stated that the periostracum covered the whole pallet in perfect specimens. Sometimes a few lateral awns were visible (Figure 9). Turner (1971b) reported lateral awns on all segments in young specimens. In older ones, the pallets became worn, chalky, scaly and they could lose the awns (Turner, 1971b). Two samples with damaged or ambiguous shaped pallets were identified as *Nototeredo sp.*.

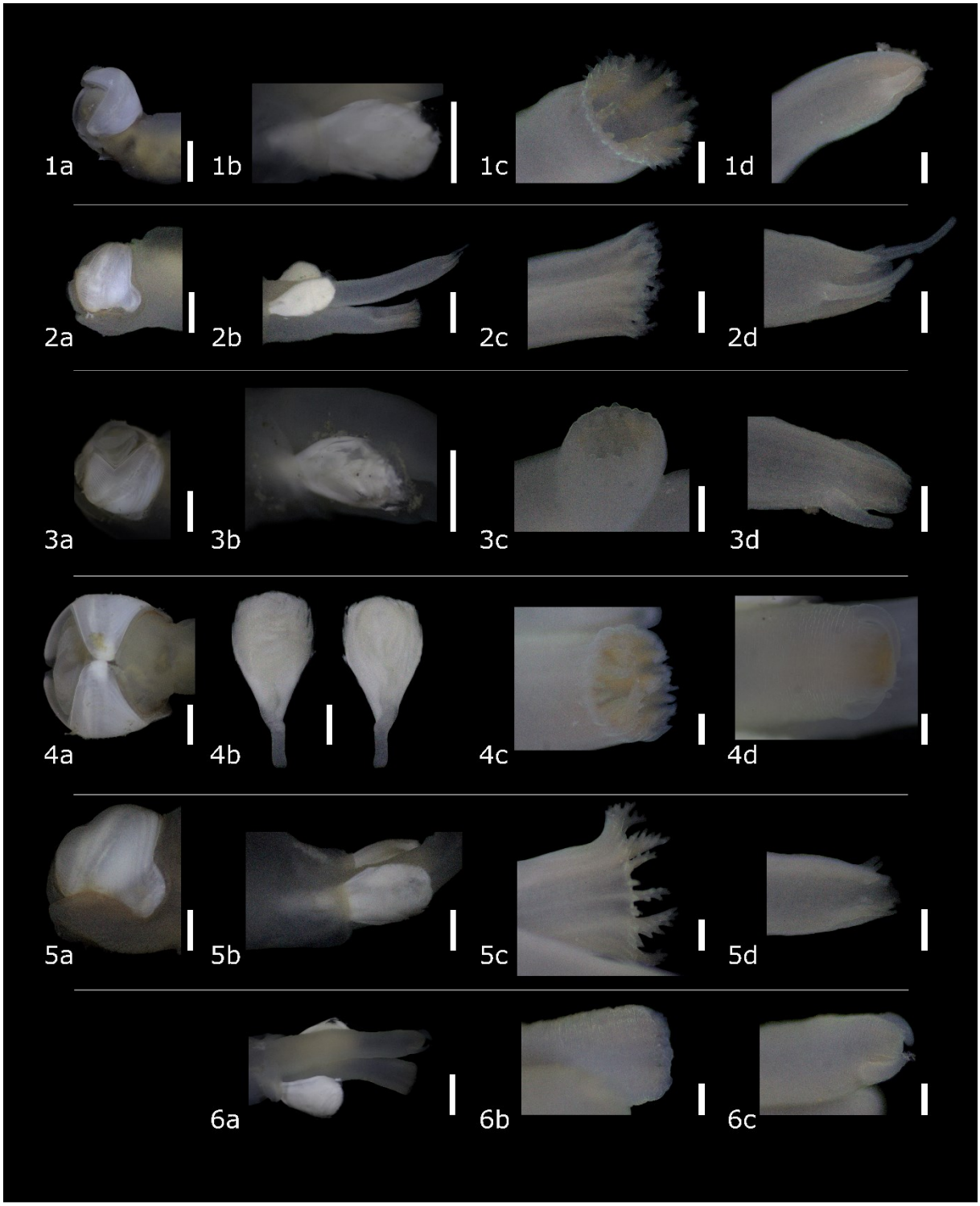

Figure 9: Micrographs of six of *Nototeredo norvagica* specimens with heads (1-5a), pallets (1-5b, 6a), incurrent siphons (1-5c, 6b) and excurrent siphons (1-5d, 6c). Scale bar (1-6a,1-5b) = 2mm, scale bar (1-5c, 1-5d, 6b,6c) = 0.5mm. The samples 6166 (1), 6530 (2), 6551(3), 6522 (4), 6561 (5) and 6266 (6) were presented here.

The third species was *Teredo bartschi.* Three specimens matched its description (Turner, 1971b). The pallets were not segmented and broadly oval to elongate. The calcareous part consisted of a single piece. The blade was composed of mostly the calcareous part. The pallet was slightly to deeply cupped. The golden to

dark brown periostracum covered the inside of the cup. It sometimes extended laterally as little horns The calcareous part did not reach the distal end but was visible inside the periostracum. The distal margin of the inner side of the pallet was U-shaped. The distal end of the outer side was U to V shaped (Figure 10).

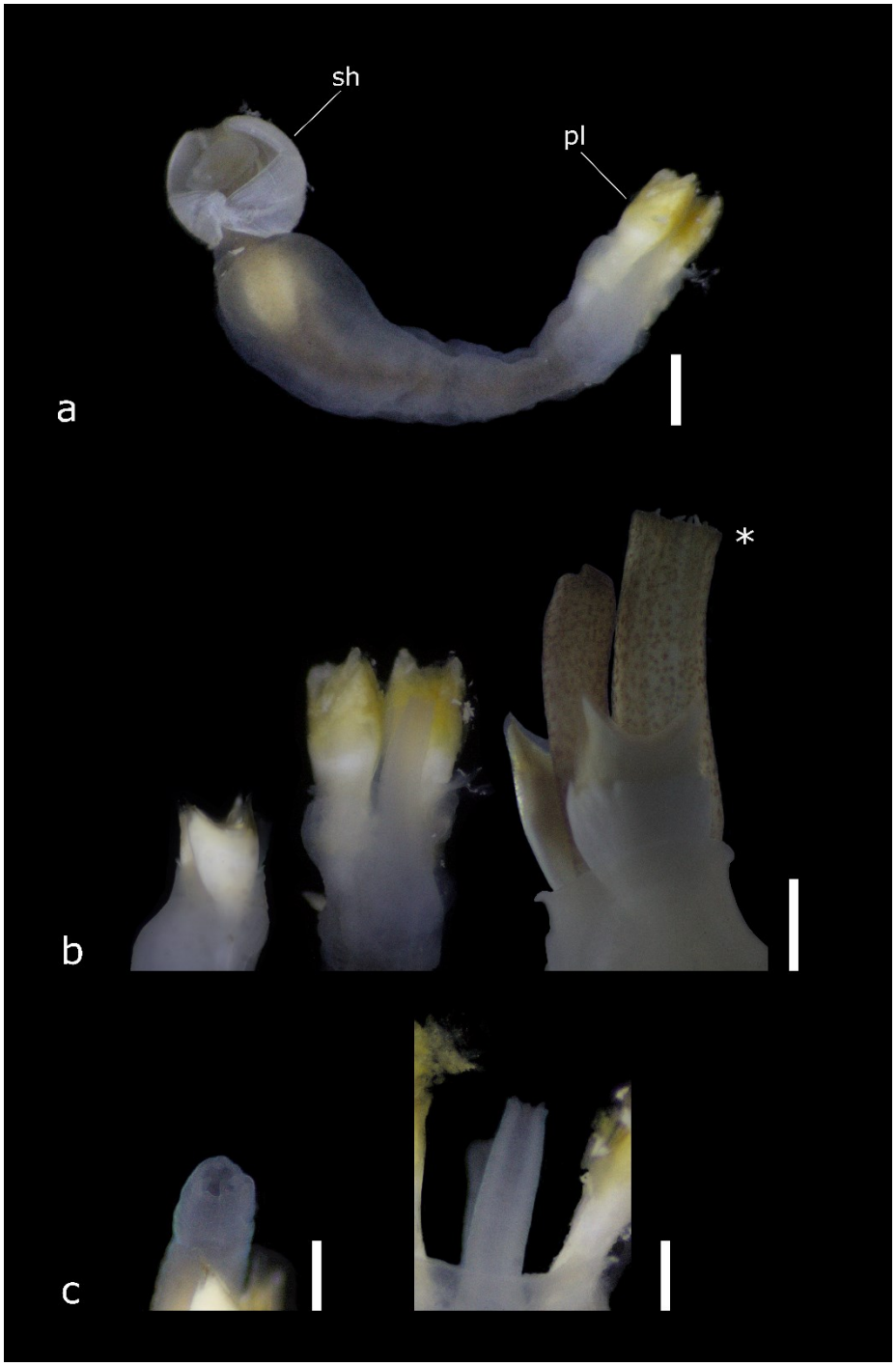

Figure 10: Micrographs of *Teredo cf. bartschi*. a) Whole specimen with shell (sh) and pallets (pl) (sample 6284), b) posterior end with pallets and siphons (*composite picture) (samples left to right: 6563; 6284; 5389), c) incurrent siphons (samples left to right: 6563; 6284). Scale bar (a, b) = 1mm, scale bar (c) = 0.5mm.

The fourth species was *Teredo navalis* with one morphologically identified specimen. The pallets were broadly oval to elongate and not segmented. The calcareous blade part constituted of a single piece. The blade was primarily the calcareous and distally cupped. The pale-yellow periostracum covered the distal half of the blade and extended only as a narrow margin. Both sides of the pallets were distally U shaped (Figure 11). There were no samples identified as *Teredo* sp.

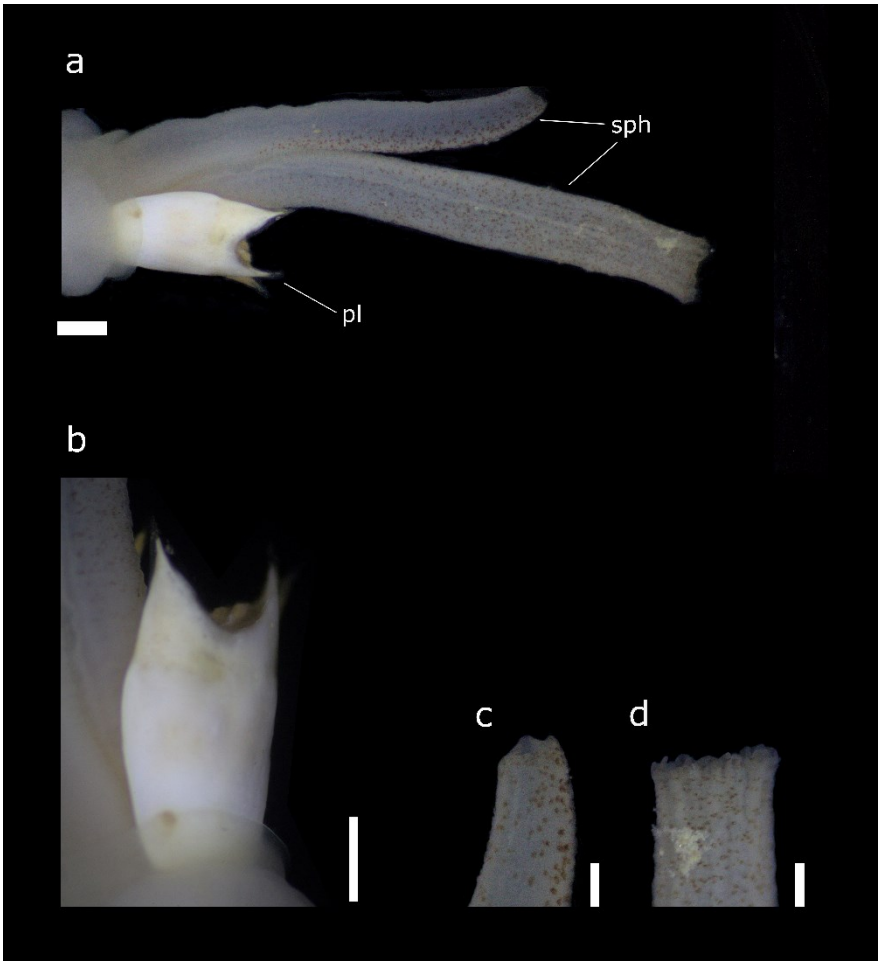

Figure 11: Micrographs of posterior end of *Teredo navalis* (a; sample: 6394) with siphons (sph) and pallets (pl). Closeups from the pallet (b.), excurrent (c.) and incurrent siphon (d.). Scale bar (a, b) = 1mm, scale bar (c, d) = 0.5mm.

Molecular identification based on 18S and additional COI sequences

The PCR products, 18S rRNA gene, of 77 samples were successfully Sanger sequenced (the samples 6295 and 6562 were very short and excluded from further analysis). The 18S phylogenetic trees were based on 75 sample sequences, plus 16 sequences from GenBank (Table 1). The sequences did not

cover the entire length of 18S rRNA gene as they missed around 100 bp at the 5'end compared to the reference sequences. Therefore, I trimmed the length of all sequences from NCBI to 1602 bp length and compared them to the 75 obtained sequences from my samples.

41 obtained sequences were identical and clustered with all *Lyrodus pedicellatus* sequences from the NCBI database, including one from the Mediterranean Sea. 12 obtained sequences were identical and clustered with all *Teredo navalis* sequences. 21 obtained sequences were identical and clustered with all *Nototeredo norvagica*. One obtained sequence, however, was the sister taxa to the *N. norvagica* cluster.

The BLAST searches resulted in members of the Teredinidae family as best hits. These were *Lyrodus pedicellatus*, *Teredo navalis* and *Nototeredo norvagica*. In the BLAST results, the difference between the species was often below one percent. The published 18S rRNA gene sequences of *Lyrodus mersinensis* in GenBank were all partial with a length of around 340 bp only. These fragments were located at the 5'end of the 18S rRNA gene sequence. This 18S region included the single position distinguishing *L. pedicellatus* and *L. mersinensis.* Therefore, I could not distinguish these two species based on the 18S sequences. Based on the COI sequences done with a subset of the dataset (Figure 18) and the geographical location, the samples were identified as *L. mersinensis.* It should be noted, however that *L. pedicellatus* (KU201123) in GenBank is from the Mediterranean as well. Its status is further reviewed in the discussion. While plenty of 18S rRNA sequences were available for *N. norvagica* and *T. navalis* in the NCBI database for comparisons, no *Teredo bartschi data* were available. Our morphologically identified specimens of *T. navalis* and *T. bartschi* cluster in our phylogenetic analysis.

Based on the tree results, the pairwise similarities were calculated with the dataset 449ex (see below). *Lyrodus pedicellatus* (JF899211) was separated from the other sequences. This was done due to its differences with the *Lyrodus pedicellatus* sequences from GenBank in the maximum likelihood trees. The samples 5389, 6284 and 6563 were identified as *Teredo cf. bartschi.* The intraspecific similarities were all 100%. If applicable, the first quartile (Q25), the median and the third quartile (Q75) were calculated. Being one sequence, no intraspecific similarity was

calculated for *L. pedicellatus* (JF899211). Similarly, the first and third quartile could not be calculated for *Bankia carinata* with only two sequences (Table 3).

Table 3: Intraspecific pairwise similarity of the taxon 1. *Lyrodus pedicellatus/mersinensis* (n=46), 2. *Lyrodus pedicellatus* (JF899211) (n=1), 3. *Teredo navalis* (n=13), 4. *Teredo cf. bartschi* (n=3), 5. *Nototeredo norvagica (*n=25) and 6. *Bankia carinata* (n=2). The first quartile (Q25), the median and the third quartile (Q75) were calculated in % (n.a.= not applicable, n=90).

	Pairwise Similarity (%)		
Taxon	**Q25**	**Median**	**Q75**
1. *Lyrodus pedicellatus/mersinensis*	100	100	100
2. *Lyrodus pedicellatus* (JF899211)	n.a.	n.a.	n.a.
3. *Teredo navalis*	100	100	100
4. *Teredo cf. bartschi*	100	100	100
5. *Nototeredo norvagica*	100	100	100
6. *Bankia carinata*	n.a.	100	n.a.

The interspecific similarity was high across the different species. *Teredo cf. bartschi* it was 100% similar to *Teredo navalis*. *Lyrodus pedicellatus/mersinensis* (*L. ped/mers.*) had with 99.94% the second highest interspecific similarity to *Teredo navalis* and *T. cf. bartschi*. *L. pedicellatus* (JF899211) was the second closest to *L. ped/mers.* with a 99.69%. *N. norvagica* was with around 98% similarity the most dissimilar. The most difference was found between *N. norvagica* and *B. carinata* with a 97.61% (Table 4).

Table 4: Interspecific pairwise similarity of the taxon 1. *Lyrodus pedicellatus/mersinensis* (n=46), 2. *Lyrodus pedicellatus* (JF899211) (n=1), 3. *Teredo navalis* (n=13), 4. *Teredo cf. bartschi* (n=3), 5. *Nototeredo norvagica (*n=25) and 6. *Bankia carinata* (n=2). The first quartile (Q25), the median and the third quartile (Q75) were calculated in % (n.a.= not applicable, n=90).

	Interspecific Pairwise Similarity (%)														
Taxon	1			2			3			4			5		
	Q25	**Median**	**Q75**	**Q25**	**Median**	**Q75**	**Q25**	**Median**	**Q75**	**Q25**	**Median**	**Q75**	**Q25**	**Median**	**Q75**
1. *L. pedicellatus/mersinensis*															
2. *L. pedicellatus* (JF899211)	99.69	99.69	99.69												
3. *T. navalis*	99.94	99.94	99.94	99.62	99.62	99.62									
4. *T. cf. bartschi*	99.94	99.94	99.94	99.62	99.62	99.62	100	100	100						
5. *N. norvagica*	98.11	98.11	98.11	97.79	97.80	97.80	98.17	98.18	98.18	98.16	98.17	98.17			
6. *B. carinata*	98.87	98.87	98.87	n.a.	98.55	n.a.	98.93	98.93	98.93	98.92	98.93	98.93	97.61	97.61	97.61

The Maximum Parsimony tree (MP) resulted in four clades with *Martesia striata* as the outgroup (Figure 12). My samples belonged to three clades, *Lyrodus pedicellatus, Teredo navalis* and *Nototeredo norvagica*. The fourth clade contained two *Bankia carinata* sequences from GenBank. *L. pedicellatus* and *T. navalis* were closest to each other. *N. norvagica* was furthest from the other clades. Here, the

sample 6545 stood out. The morphological *Lyrodus cf. mersinensis* and *Lyrodus sp.* were in the *L. pedicellatus* clade. The morphospecies *T. navalis* and *T. bartschi* were not distinguished in the MP. They were both in the *T. navalis* cluster. The morphologically *N. norvagica* and *Nototeredo sp.* samples were in the *N. norvagica* cluster.

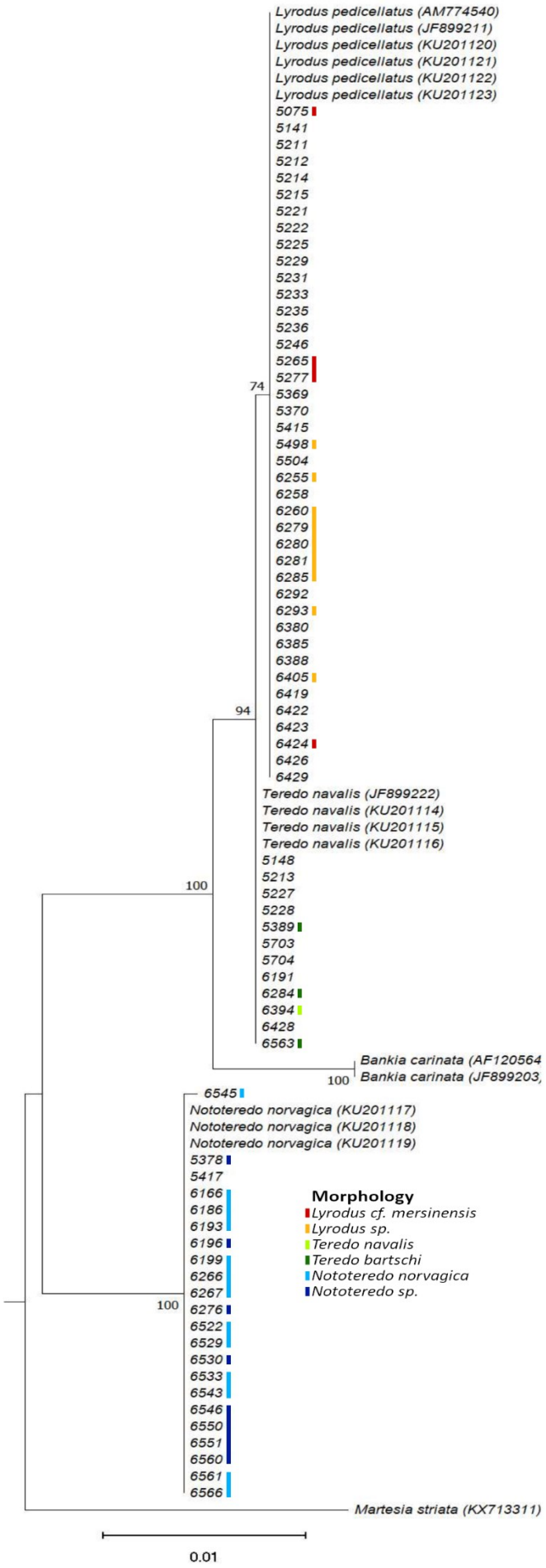

Figure 12*:* Maximum Parsimony tree (18S rRNA) with morphology results. Bootstrap support values under 50% are not shown. Morphology in colours with *Lyrodus cf. mersinensis* (red), *Lyrodus sp.* (orange), *Teredo navalis* (green), *Teredo bartschi* (dark green), *Nototeredo norvagica* (blue), *Nototeredo sp.* (dark blue) (n= 91).

Sample 6545 differed in two nucleotides from the other sequences in its clade. The chromatogram revealed the two differentiating positions at 119 and 225 (Figure 13). The position 119 was an adenine (A) instead of a guanine (G) like the other sequences. The position 125 had a cytosine (C) instead of a thymine (T). The two positions showed a weak signal in the chromatogram (Figure 2). In the final alignment these positions were 131 and 137.

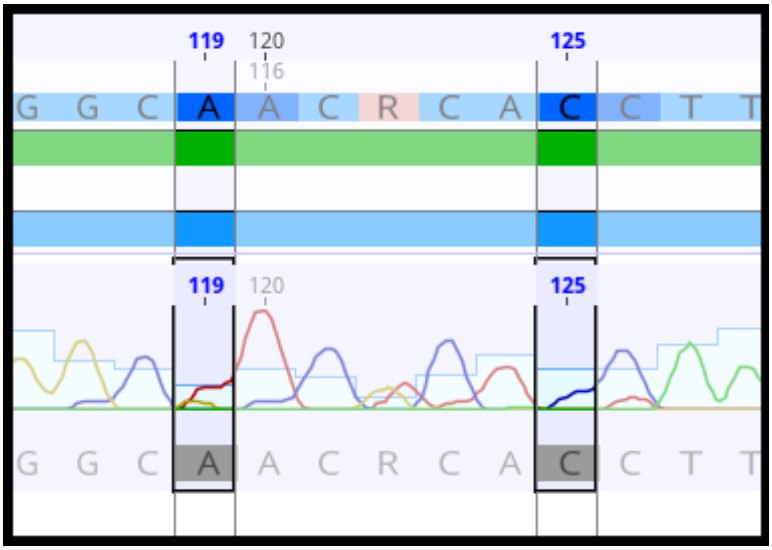

Figure 13: Chromatogram of the sample 6545 with the two highlighted positions being the difference to the other *Nototeredo norvagica* samples.

The Maximum Likelihood tree (ML) was similar to the MP but contained more differentiation. These different nodes have bootstrap values of under 50%. *Lyrodus pedicellatus* (JF899211) differed from the other GenBank sequences. The samples 5415, 6255 and 6292 were separated from the other *L. pedicellatus* in the cluster. Next to the *L. pedicellatus* cluster was the *Teredo navalis* cluster. Here 11 sequences, from the *L. pedicellatus* cluster in MP were placed closer to *T. navalis* than *L. pedicellatus.* These were the only samples that were in a different cluster compared to the MP tree. In the *Nototeredo norvagica* cluster, the sample 6545 stood out as in the previous tree. *N. norvagica* had one subdivision (Figure 14).

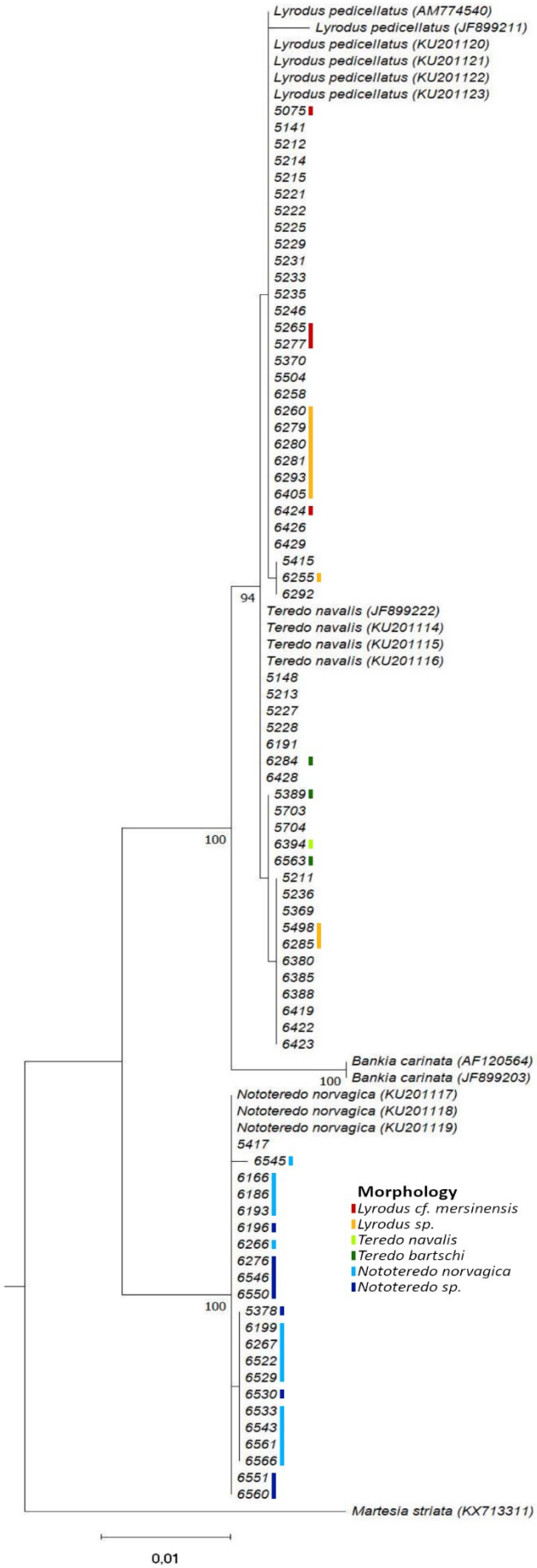

Figure 14: Maximum Likelihood (18S rRNA) with morphology results. Bootstrap support values under 50% are not shown. Morphology represented in colours with *Lyrodus cf. mersinensis* (red), *Lyrodus sp.* (orange), *Teredo navalis* (green), *Teredo bartschi* (dark green), *Nototeredo norvagica* (blue), *Nototeredo sp.* (dark blue) (n= 91).

I checked for a possible cause for the MP and ML differences. In the sequence alignment, the position 449 stood out. In the reference sequences from GenBank this position was always a thymine. In our sequences this was not the case. It could be adenine, thymine or ambiguous. In the chromatograms I saw that position 449 was weird. In best case it had a weak thymine signal (Figure 15 a, b). In others the thymine signal was non- existent and Sanger sequencing identified the position with a very weak signal as adenine (Figure 15 c, d). To avoid problems deriving from position 449, I excluded it and created a second dataset (449ex). I redid both trees with dataset 449ex to see its effects. The new Maximum Parsimony tree (MP 449ex) was, despite of some bootstrap values, identical to MP (Figure 16). The new Maximum Likelihood tree (ML 449ex) differed from the previous ML. It resembled instead MP with one difference prevailing. Lyrodus pedicellatus (JF899211) stood out against the other sequences in the Lyrodus pedicellatus cluster (Figure 17). The alignment showed different nucleotides at five positions compared to the L. pedicellatus references.

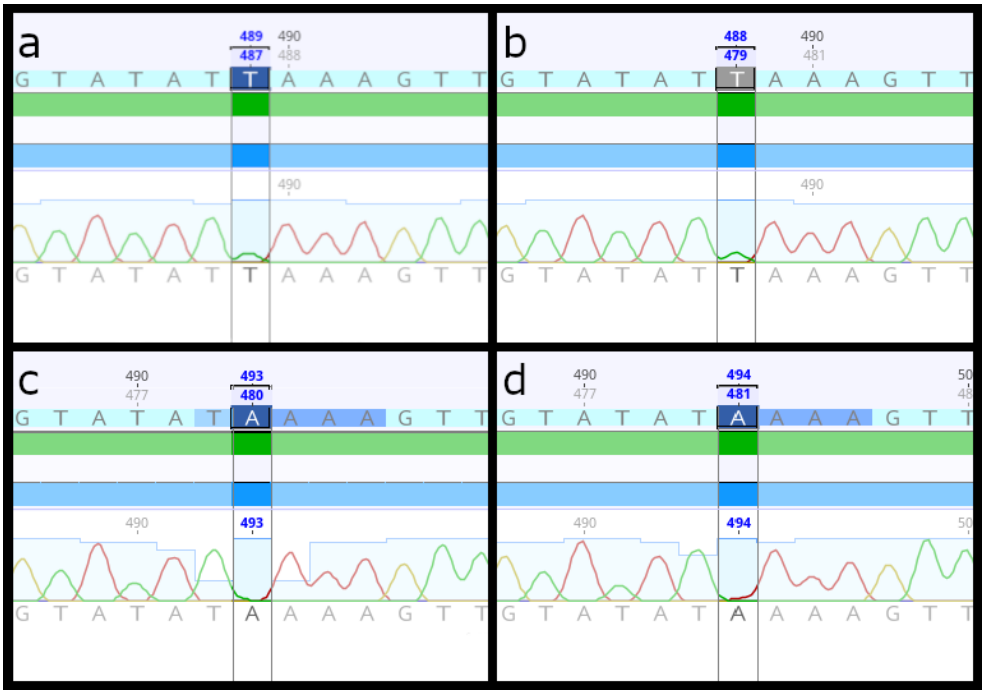

Figure 15: Chromatograms showing the position 449 (before alignment) with samples 5212 (a), 6260 (b), 6380 (c) and 6533 (d). In a and b thymine was identified correctly. In c and d this position was identified incorrectly as adenine. Note that the position before and after the alignment may differ (n=4).

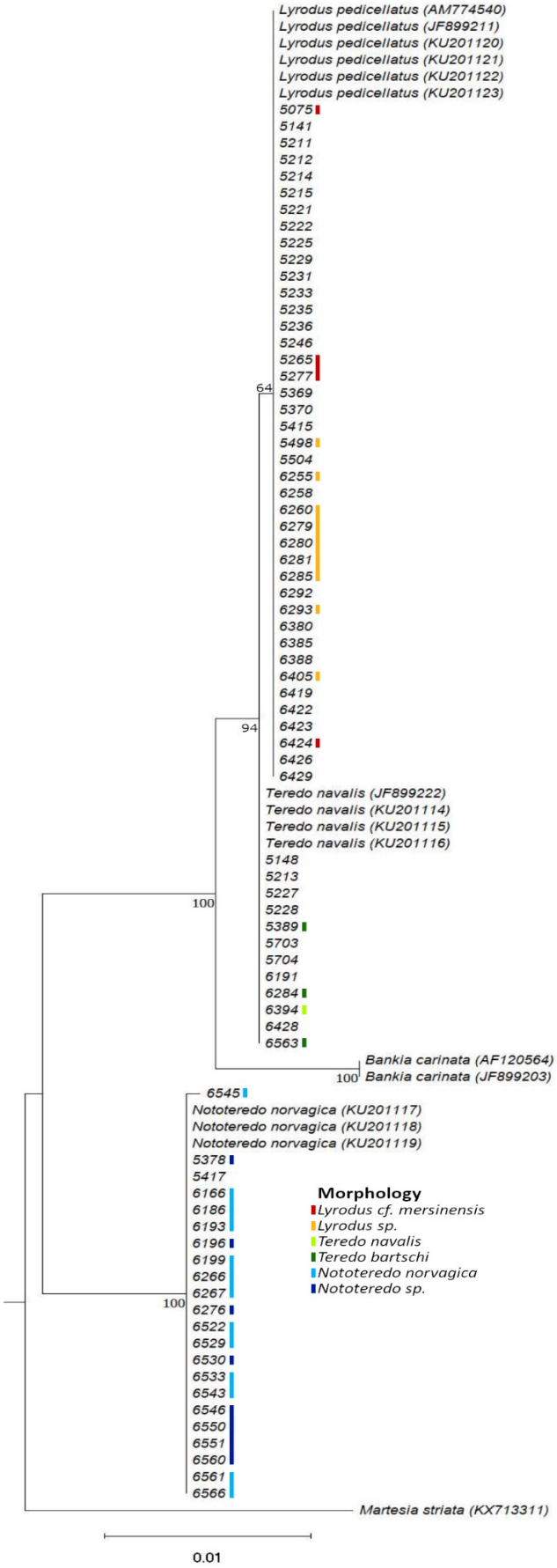

Figure 16: Maximum Parsimony tree of the dataset 449ex (18S rRNA) including morphology results. Bootstrap support values under 50% are not shown. Morphology represented in colours with *Lyrodus cf. mersinensis* (red), *Lyrodus sp.* (orange), *Teredo navalis* (green), *Teredo bartschi* (dark green), *Nototeredo norvagica* (blue), *Nototeredo sp.* (dark blue) (n= 91).

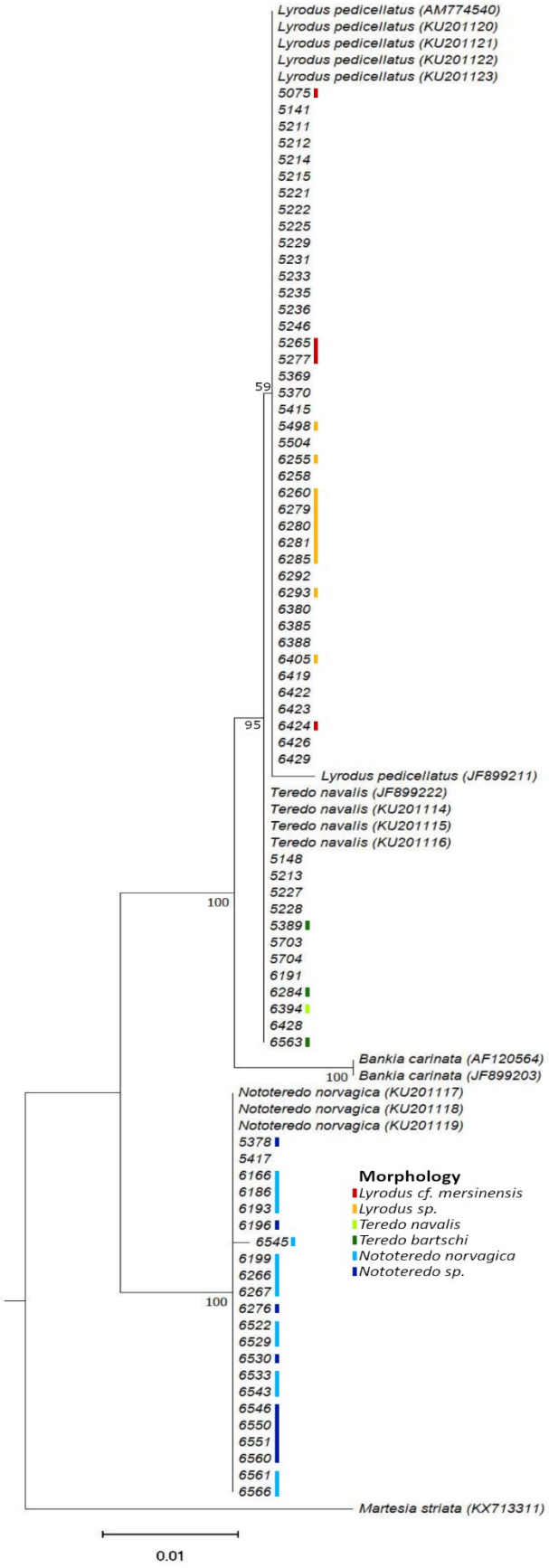

Figure 17: Maximum Likelihood tree with the dataset 449ex (18S rRNA) including morphology results. Bootstrap support values under 50% are not shown. Morphology represented in colours with *Lyrodus cf. mersinensis* (red), *Lyrodus sp.* (orange), *Teredo navalis* (green), *Teredo bartschi* (dark green), *Nototeredo norvagica* (blue), *Nototeredo sp.* (dark blue) (n= 91).

The BLAST searches for the COI sequences resulted in *Lyrodus mersinensis, Teredo navalis* and *Nototeredo norvagica* as best hits. The maximum likelihood tree using the COI shipworm sequences grouped our samples into three clades (Figure 18). The first clade was *T. navalis* with the *Teredo bartschi* reference (NC_063766.1) as sister taxon. The morphospecies *T. cf. bartschi* and *T. navalis* were clustered together. The second clade was *N. norvagica* with sample 6545 standing out. The third clade was *L. mersinensis* with *Lyrodus pedicellatus* as sister taxon. The morphospecies *N. norvagica* and *L. mersinensis* aligned with the phylogenetic tree.

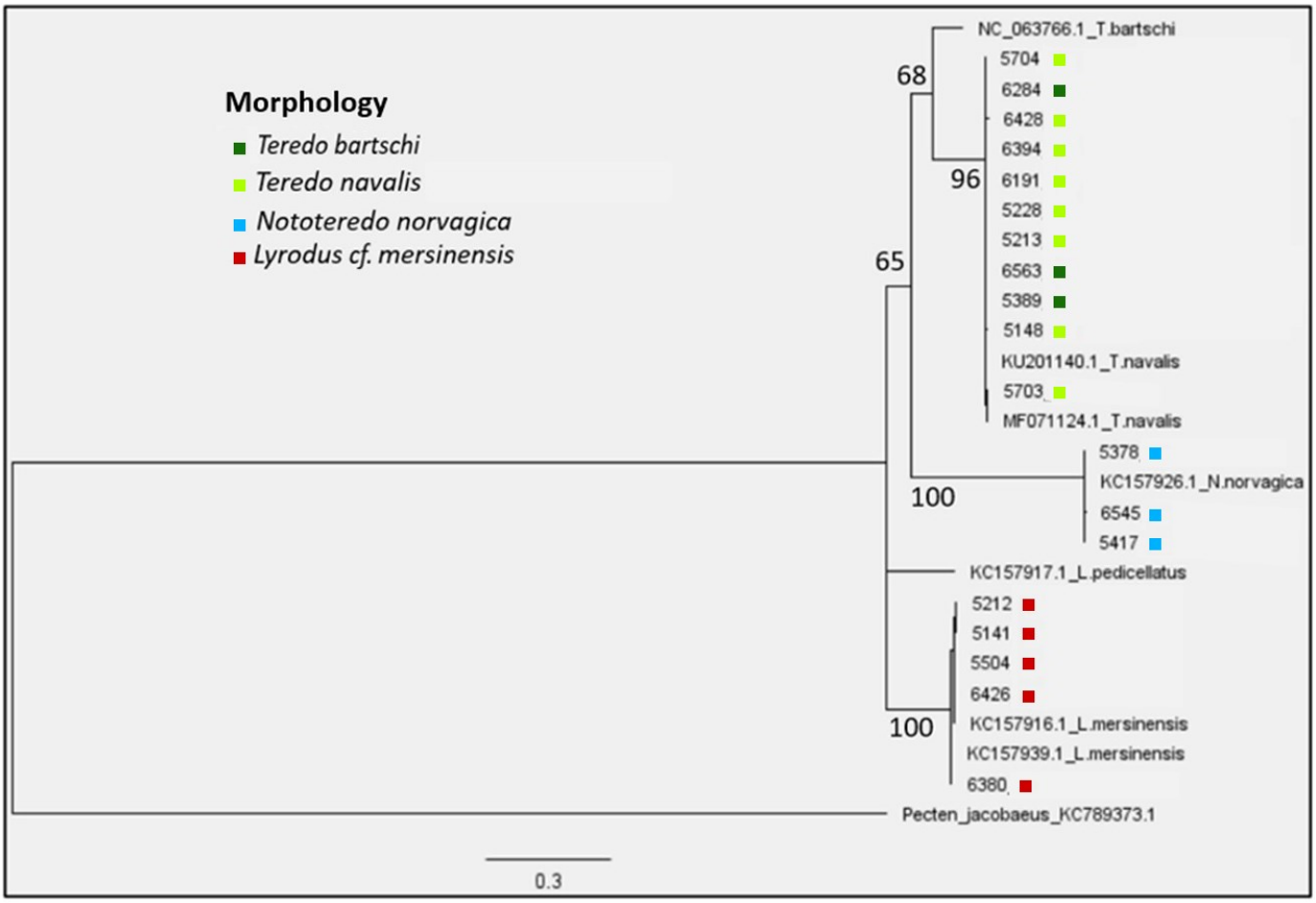

Figure 18. Maximum Likelihood tree of shipworm COI sequences with bootstrap support values and morphology. Bootstrap support values under 50% are not shown. Morphology represented in colours with *Teredo cf. bartschi* (dark green), *Teredo navalis* (green), *Nototeredo norvagica* (blue) and *Lyrodus mersinensis* (red) (n= 27) (Courtesy: Gaëlle Berte).

Final identification

The 18S and COI sequence results were put against the morphospecies. This resulted in the final identification of the three species *Lyrodus mersinensis, Teredo navalis* and *Nototeredo norvagica.*

Table 5: Identity of our shipworms with vial number, sampling site, collection date, cube, plate, plus morphological and 18S rRNA identification. The asterisks mark samples with an additional COI sequence.

Species name (*COI)	Vial number	Site	Cube & plate	Collection date	Morphology	18S rRNA
Lyrodus mersinensis	5075	Institute	5	17.02.2020	*Lyrodus cf. mersinensis*	*Lyrodus pedicellatus*
*Lyrodus mersinensis**	5141	Strunjan	9 Sub	20.02.2020	/	*Lyrodus pedicellatus*
*Teredo navalis**	5148	Strunjan	9 B	20.02.2020	/	*Teredo navalis*
Lyrodus mersinensis	5211	Institute	13	15.07.2020	/	*Lyrodus pedicellatus*
*Lyrodus mersinensis**	5212	Institute	13	15.07.2020	Teredinidae	*Lyrodus pedicellatus*
*Teredo navalis**	5213	Institute	13	15.07.2020	Teredinidae	*Teredo navalis*
Lyrodus mersinensis	5214	Institute	13	15.07.2020	Teredinidae	*Lyrodus pedicellatus*
Lyrodus mersinensis	5215	Institute	13	15.07.2020	Teredinidae	*Lyrodus pedicellatus*
Lyrodus mersinensis	5221	Institute	13D	15.07.2020	Teredinidae	*Lyrodus pedicellatus*
Lyrodus mersinensis	5222	Institute	13D	15.07.2020	Teredinidae	*Lyrodus pedicellatus*
Lyrodus mersinensis	5225	Institute	13B	15.07.2020	/	*Lyrodus pedicellatus*
Teredo navalis	5227	Institute	13B	15.07.2020	/	*Teredo navalis*
*Teredo navalis**	5228	Institute	13B	15.07.2020	/	*Teredo navalis*
Lyrodus mersinensis	5229	Institute	13B	15.07.2020	Teredinidae	*Lyrodus pedicellatus*
Lyrodus mersinensis	5231	Institute	13B	15.07.2020	/	*Lyrodus pedicellatus*
Lyrodus mersinensis	5233	Institute	13F	15.07.2020	/	*Lyrodus pedicellatus*
Lyrodus mersinensis	5235	Institute	13F	15.07.2020	/	*Lyrodus pedicellatus*
Lyrodus mersinensis	5236	Institute	13F	15.07.2020	/	*Lyrodus pedicellatus*
Lyrodus mersinensis	5246	Institute	13F	15.07.2020	/	*Lyrodus pedicellatus*
Lyrodus mersinensis	5265	Institute	13 Sub	19.07.2020	*Lyrodus cf. mersinensis*	*Lyrodus pedicellatus*
Lyrodus mersinensis	5277	Institute	14	19.07.2020	*Lyrodus cf. mersinensis*	*Lyrodus pedicellatus*
Lyrodus mersinensis	5369	Institute	17A	25.07.2020	/	*Lyrodus pedicellatus*
Lyrodus mersinensis	5370	Institute	17A	25.07.2020	/	*Lyrodus pedicellatus*
*Nototeredo norvagica**	5378	Institute	17A	25.07.2020	*Nototeredo norvagica*	*Nototeredo norvagica*
*Teredo navalis**	5389	Institute	17D	26.07.2020	*Teredo bartschi*	*Teredo navalis*

Lyrodus mersinensis	5415	Strunjan	18E	27.07.2020	/	*Lyrodus pedicellatus*
*Nototeredo norvagica**	5417	Strunjan	18E	27.07.2020	Teredinidae	*Nototeredo norvagica*
Lyrodus mersinensis	5498	Strunjan	22B	06.08.2020	*Lyrodus sp.*	*Lyrodus pedicellatus*
*Lyrodus mersinensis**	5504	Strunjan	22B	06.08.2020	/	*Lyrodus pedicellatus*
*Teredo navalis**	5703	Institute	27	17.08.2020	/	*Teredo navalis*
*Teredo navalis**	5704	Institute	27	17.08.2020	/	*Teredo navalis*
Nototeredo norvagica	6166	Institute	28A	09.03.2021	*Nototeredo norvagica*	*Nototeredo norvagica*
Nototeredo norvagica	6186	Institute	28A	09.03.2021	*Nototeredo norvagica*	*Nototeredo norvagica*
*Teredo navalis**	6191	Institute	28 Sub	09.03.2021	Teredinidae	*Teredo navalis*
Nototeredo norvagica	6193	Institute	28 Sub	09.03.2021	*Nototeredo norvagica*	*Nototeredo norvagica*
Nototeredo norvagica	6196	Institute	28 Sub	09.03.2021	*Nototeredo sp.*	*Nototeredo norvagica*
Nototeredo norvagica	6199	Institute	28 Sub	09.03.2021	*Nototeredo norvagica*	*Nototeredo norvagica*
Lyrodus mersinensis	6255	Institute	29C	12.03.2021	*Lyrodus sp.*	*Lyrodus pedicellatus*
Lyrodus mersinensis	6258	Institute	29A	12.03.2021	Teredinidae	*Lyrodus pedicellatus*
Lyrodus mersinensis	6260	Institute	29A	12.03.2021	*Lyrodus sp.*	*Lyrodus pedicellatus*
Nototeredo norvagica	6266	Institute	29 Sub	12.03.2021	*Nototeredo norvagica*	*Nototeredo norvagica*
Nototeredo norvagica	6267	Institute	29 Sub	12.03.2021	*Nototeredo norvagica*	*Nototeredo norvagica*
Nototeredo norvagica	6276	Institute	30 Sub	12.03.2021	*Nototeredo norvagica*	*Nototeredo norvagica*
Lyrodus mersinensis	6279	Institute	29B	12.03.2021	*Lyrodus sp.*	*Lyrodus pedicellatus*
Lyrodus mersinensis	6280	Institute	29B	12.03.2021	*Lyrodus sp.*	*Lyrodus pedicellatus*
Lyrodus mersinensis	6281	Institute	29B	12.03.2021	*Lyrodus sp.*	*Lyrodus pedicellatus*
*Teredo navalis**	6284	Institute	30D	12.03.2021	*Teredo bartschi*	*Teredo navalis*
Lyrodus mersinensis	6285	Institute	30E	12.03.2021	*Lyrodus sp.*	*Lyrodus pedicellatus*
Lyrodus mersinensis	6292	Institute	29D	12.03.2021	Teredinidae	*Lyrodus pedicellatus*
Lyrodus mersinensis	6293	Institute	29D	12.03.2021	*Lyrodus sp.*	*Lyrodus pedicellatus*
Lyrodus sp.	6295	Institute	29D	12.03.2021	*Lyrodus sp.*	/
*Lyrodus mersinensis**	6380	Lera	34 Sub	15.03.2021	/	*Lyrodus pedicellatus*
Lyrodus mersinensis	6385	Lera	34D	15.03.2021	Teredinidae	*Lyrodus pedicellatus*
Lyrodus mersinensis	6388	Lera	34E	15.03.2021	/	*Lyrodus pedicellatus*
*Teredo navalis**	6394	Lera	34	15.03.2021	*Teredo navalis*	*Teredo navalis*
Lyrodus mersinensis	6405	Lera	34D	15.03.2021	*Lyrodus sp.*	*Lyrodus pedicellatus*
Lyrodus mersinensis	6419	Lera	32	15.03.2021	/	*Lyrodus pedicellatus*
Lyrodus mersinensis	6422	Lera	34B	15.03.2021	/	*Lyrodus pedicellatus*

Lyrodus mersinensis	6423	Lera	34D	15.03.2021	Teredinidae	*Lyrodus pedicellatus*
Lyrodus mersinensis	6424	Lera	34D	15.03.2021	*Lyrodus cf. mersinensis*	*Lyrodus pedicellatus*
*Lyrodus mersinensis**	6426	Lera	34C	15.03.2021	Teredinidae	*Lyrodus pedicellatus*
*Teredo navalis**	6428	Lera	33C	15.03.2021	Teredinidae	*Teredo navalis*
Lyrodus mersinensis	6429	Lera	33F	15.03.2021	Teredinidae	*Lyrodus pedicellatus*
Nototeredo norvagica	6522	Strunjan	36 Sub	19.03.2021	*Nototeredo norvagica*	*Nototeredo norvagica*
Nototeredo norvagica	6529	Strunjan	36 Sub	19.03.2021	*Nototeredo norvagica*	*Nototeredo norvagica*
Nototeredo norvagica	6530	Strunjan	36 Sub	19.03.2021	*Nototeredo sp.*	*Nototeredo norvagica*
Nototeredo norvagica	6533	Strunjan	36 Sub	19.03.2021	*Nototeredo norvagica*	*Nototeredo norvagica*
Nototeredo norvagica	6543	Strunjan	39 Sub	19.03.2021	*Nototeredo norvagica*	*Nototeredo norvagica*
*Nototeredo norvagica**	6545	Strunjan	38 Sub	19.03.2021	*Nototeredo norvagica*	*Nototeredo norvagica*
Nototeredo norvagica	6546	Strunjan	38 Sub	19.03.2021	*Nototeredo norvagica*	*Nototeredo norvagica*
Nototeredo norvagica	6550	Strunjan	38	19.03.2021	*Nototeredo norvagica*	*Nototeredo norvagica*
Nototeredo norvagica	6551	Strunjan	38	19.03.2021	*Nototeredo sp.*	*Nototeredo norvagica*
Nototeredo norvagica	6560	Strunjan	36 Sub	19.03.2021	*Nototeredo norvagica*	*Nototeredo norvagica*
Nototeredo norvagica	6561	Strunjan	36 Sub	19.03.2021	*Nototeredo norvagica*	*Nototeredo norvagica*
Lyrodus mersinensis	6562	Strunjan	36B	19.03.2021	*Lyrodus cf. mersinensis*	/
*Teredo navalis**	6563	Strunjan	36B	19.03.2021	*Teredo bartschi*	*Teredo navalis*
Nototeredo norvagica	6566	Strunjan	36B	19.03.2021	*Nototeredo norvagica*	*Nototeredo norvagica*

Ecological analysis

Over the three-year project 50 wood cubes were collected. In Lera it was 18 cubes. In Strunjan 15 cubes were sampled. In Institute 17 cubes were collected. In Institute some and in Strunjan all cubes were found completely degraded in the last sampling stay, leading to less cubes overall. In Summer 2020 an additional wood cube was collected in Institute. In Strunjan and Institute the three species were present. Lera had the two species *Lyrodus mersinensis* and *Teredo navalis*. *Nototeredo norvagica* was not found in Lera. Various organisms settled during the three years on the BORG's. Most rapid overgrowth was found in Lera (Figure 19). After half a year it was already overgrown a lot so that the individual cubes became difficult to distinguish. In winter 2022 it was still standing, but its former structure was not recognisable anymore. Here ascidians dominated. Strunjan was less colonised than Lera. Here the cubes were after half a year still easily

distinguishable. In summer 2022, the cube remained had fallen apart leaving only the cable ties on the metal frame. Institute showed the least overgrowth over time. Here the overgrowth resulted in hard structures outlasting the wood (Figure 19).

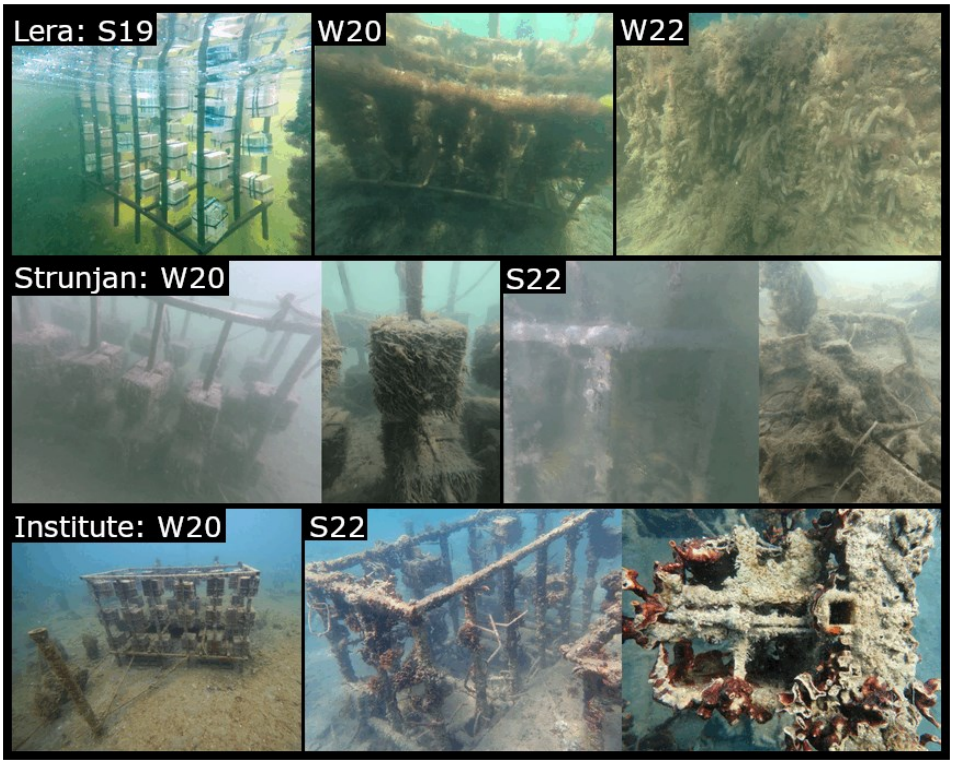

Figure 19: Pictures of the BORG's at Lera, Strunjan and Institute during different sampling stays with summer 2019 (S19), winter 2020 (W20), winter 2022 (W22) and summer 2022 (S22) (©Bright Lab).

The wood degradation speed and shipworm abundance differed between the sites (Figure 19/20). The cubes in Lera degraded very slow and contained the least amount of shipworm tunnels. The degradation speed of the cubes was higher in Institute. The plates in Strunjan and Institute contained a lot of shipworm tunnels. In Strunjan the wood degraded the fastest. After three years there was no wood left in Strunjan and only one wood plate in Institute (Figure 20).

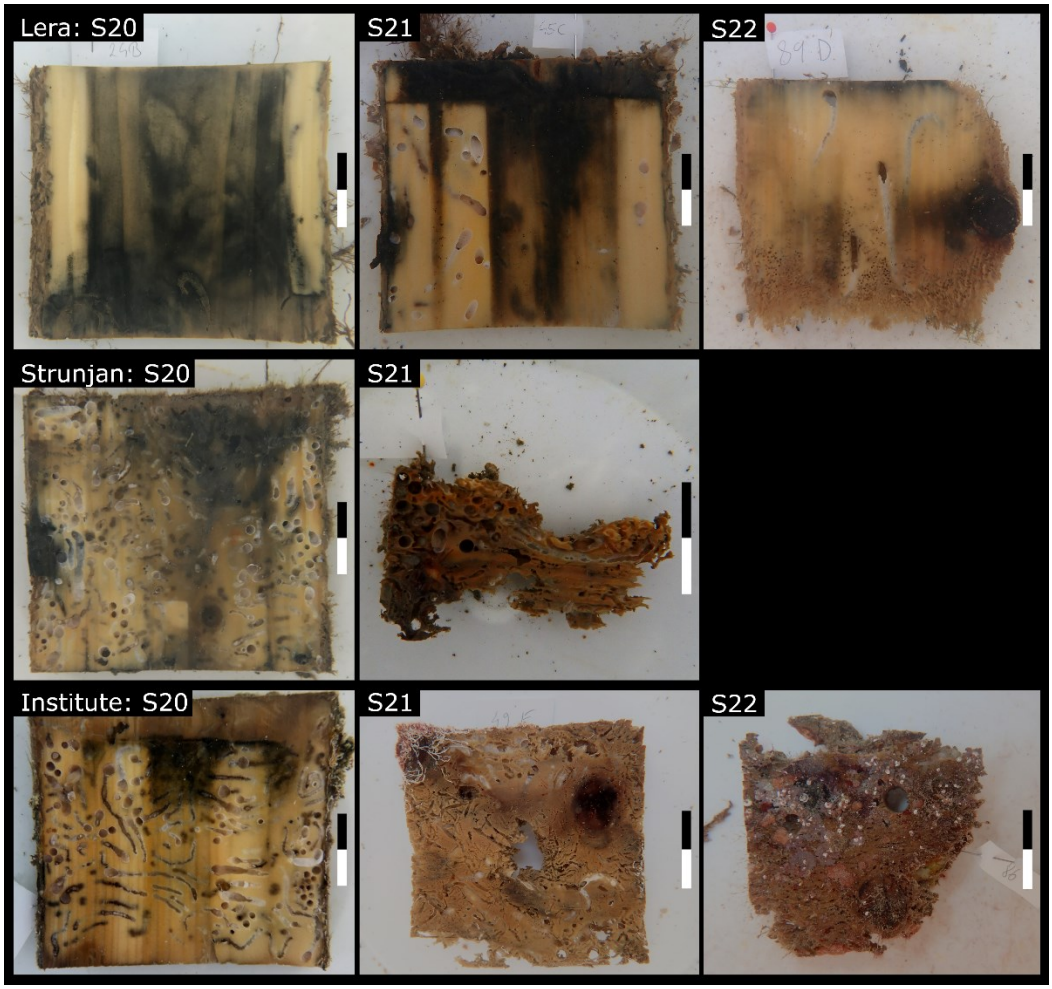

Figure 20: Wood degradation of outside cube plates over three years with summer 2020 (S20), summer 2021 (S21) and summer 2022 (S22) after the deployment in summer 2019 at Lera, Strunjan and Institute. The cube plates (S20), 45C (S21), 89D (S22) from Lera, 15C (S20), 41E (S21) from Strunjan), 14C (S20), 49E (S21) and 86 (S22) from Institute are shown. The number represents the cube and the letter the plate. Scalebar = 3cm (©Bright Lab).

The number of colonised cubes over time followed a unimodal distribution (Figure 21). *Lyrodus mersinensis* colonised all sites in the first half year. It stayed present for two years in Lera and Institute. In Strunjan *L. mersinensis* stayed a season longer. Colonization of *Teredo navalis* was more inconsistent. In Lera it was present in the second and third winter only. In Strunjan *T. navalis* appeared in the first and second winter. It colonized Institute in the first half year like *L. mersinensis* and stayed until the second winter and reappeared in the last winter. *Nototeredo norvagica* colonized Strunjan and Institute one year after deployment and was present until the last winter at both sites (Table 6).

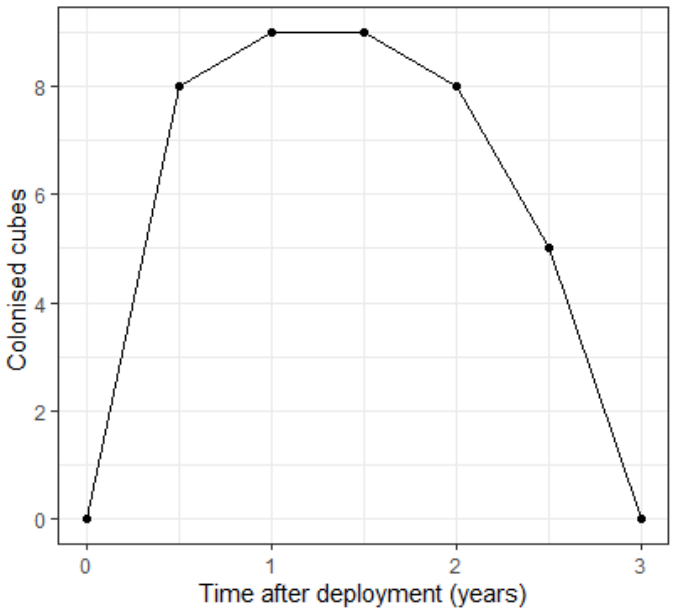

Figure 21: Number of colonised cubes from the three sites combined over three years. A maximum of nine wood cubes per sampling stay are represented.

Table 6: Presence of the species *Lyrodus mersinensis, Teredo navalis* and *Nototeredo norvagica* at the three sites Lera, Strunjan and Institute at each sampling stay.

Lera	W	S	W	S	W	S
Lyrodus mersinensis						
Teredo navalis						
Nototeredo norvagica						
Strunjan	W	S	W	S	W	S
Lyrodus mersinensis						
Teredo navalis						
Nototeredo norvagica						
Institute	W	S	W	S	W	S
Lyrodus mersinensis						
Teredo navalis						
Nototeredo norvagica						

Studying the time of colonization over time at each site, we saw that *Lyrodus mersinensis* and *Nototeredo norvagica* were well established. If present, both species were on several cubes for multiple seasons. In Institute, *Teredo navalis* had a strong start in winter 2020 with a steady decline thereafter with a re-appearance in winter 2022. In Lera and Strunjan *T. navalis* was found in some winters but not during summer (Table 7).

Table 7: Number of colonised cubes for the three identified species at the three sites Lera, Strunjan and Institute over three years. In Summer 2020 a fourth cube was collected in Institute.

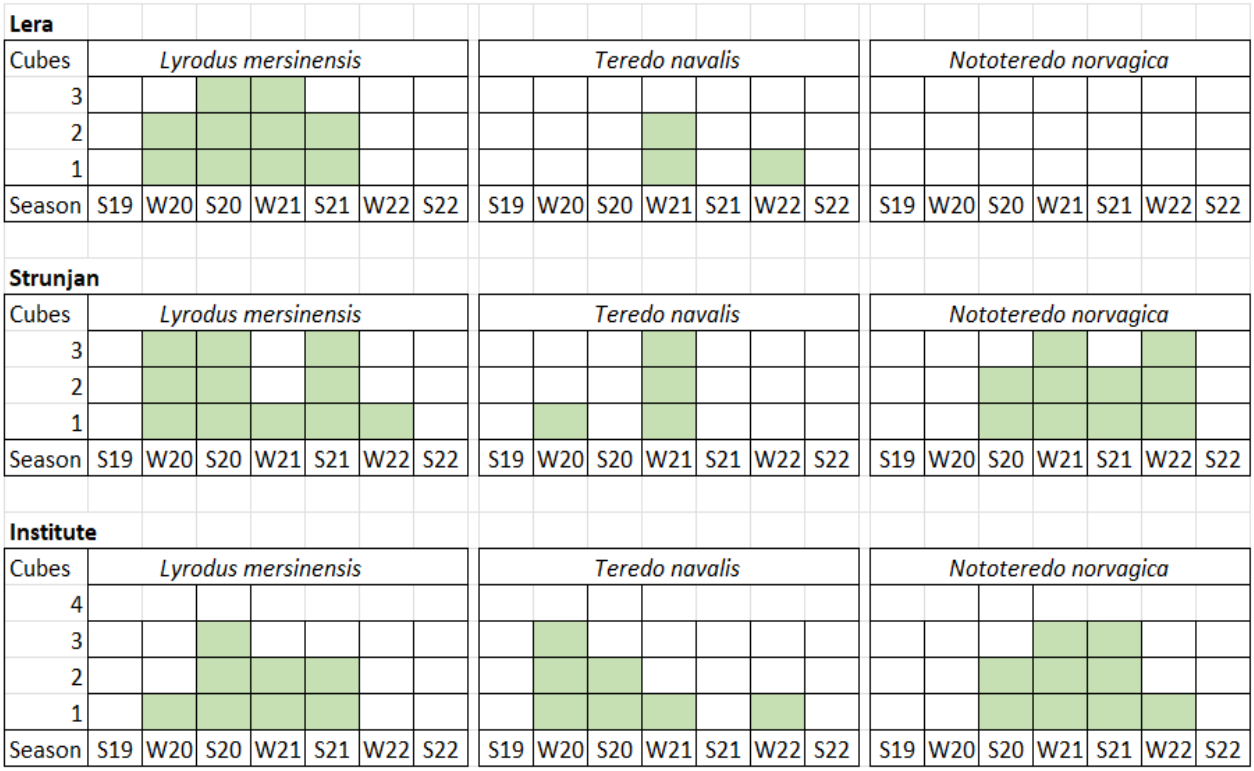

The temperature in the water surrounding the BORGs ranged from 8.0-27.8°C in Lera, 8.2-28.8°C in Strunjan and 10.0-28.1°C in Institute. The salinity ranged from 34.0-37.2 in Lera, 34.0-37.7 in Strunjan and 34.0-37.0 in Institute. The abiotic parameters of the cube insides were similar at all our sites. The biggest differences were found in the hydrogen sulphide concentrations (H_2S). After half a year Strunjan had the highest H_2S out of the three sites. But half a year later and onwards Lera had by far the highest H_2S concentration. Institute had the lowest H_2S concentration. Strunjan and Institute had high increase in dissolved oxygen saturation (DOS) in the last two sampling stays. The last retrieved cubes of Strunjan had almost no H_2S. The lowest pH was measured in Lera (Table 8). The spearman correlation showed no significant influence of the presence of the three species on each other. Site showed significance for the presence of *Nototeredo norvagica*. *Teredo navalis* was significantly more present in during winter. *T. navalis* presence was negatively correlated by temperature, in accordance with the season. Salinity was significantly negative correlated with *Lyrodus mersinensis*. We measured less DOS and pH in summer. In summer we also measured more

H_2S. DOS correlated positively with pH and negatively with temperature. In contrast H_2S correlated positively with temperature (Table 9).

Table 8: Physical parameters of the cube insides for each site per season. Time after deployment (Post dep.) in years, individual cube numbers, median and minimum(min) dissolved oxygen saturations (DOS) in %, median and minimum pH, median, minimum winter- and maximum (max) summer temperatures (T) in °C, median salinity in ‰, median and maximum sulphide (H2S) in µmol. The measurements of the first year after deployment belong to cubes deployed in summer 2021 (marked with *). These are not cubes that shipworms were sampled from.

	Winter			Summer			Winter			Summer			Winter			Summer	
Sites	L	S	I	L	S	I	L	S	I	L	S	I	L	S	I	L	I
Post dep. (years)	0.5*	0.5*	0.5*	1*	1*	1*	1.5	1.5	1.5	2	2	2	2.5	2.5	2.5	3	3
Cube numbers	62; 63; 64	57; 58; 59	54; 70; 71	85; 91; 92	74; 78; 79	75; 76; 77	32; 33; 35	36; 38; 39	28; 29; 31	42; 45; 51	41; 44; 46; 48	40; 43; 49	60; 61; 70	55; 65; 66	53; 67; 68	84; 89; 90	86
DOS (%) (Median)	10	10	12	0	0	0	3	7	/	1	2	4	4	71	57	0	113
DOS (%) (min)	4	2	3	0	0	0	2	1	88	1	1	1	1	60	25	0	113
pH (Median)	8.0	8.1	8.0	7.9	7.8	7.8	7.7	7.9	8.0	7.6	7.8	8.0	8.0	8.1	8.1	7.9	8.1
pH (min)	7.9	8.1	8.0	7.8	7.7	7.8	7.7	7.8	8.0	7.5	7.8	7.9	7.9	8.1	7.9	7.9	8.1
T (°C) (Median)	11.5	9.1	11.5	23.7	26.2	27.0	13.5	13.0	12.1	25.5	27.1	25.2	9.7	11.1	9.9	23.6	23.3
Winter T (°C) (min)	10.5	8.8	10.1	/	/	/	12.9	12.4	12.0	/	/	/	9.2	11.0	9.4	/	/
Summer T (°C) (max)	/	/	/	26.7	26.7	27.6	/	/	/	25.9	27.2	25.6	/	/	/	26.7	23.3
Salinity (‰) (Median)	36.0	36.3	36.9	37.1	36.6	36.1	35.9	35.2	37.1	35.6	34.1	34.0	36.0	36.6	36.6	37.1	36.5
H2S (µmol) (Median)	3	28	3	161	107	6	74	34	4	134	36	2	39	2	1	386	0
H2S (µmol) (max)	3	59	4	533	121	14	83	222	35	425	65	3	59	2	1	435	0

Table 9: Spearman correlation of abiotic and biotic parameters. These abiotic parameters include the sites with Lera=0, Institute=1 and Strunjan=2; season with winter=0 and summer=1; time after deployment (Post_dep); dissolved oxygen saturation (DOS); pH; temperature (T°); salinity and hydrogen sulphide (H2S). The biotic parameters are the presence/absence of the species *Lyrodus mersinensis (1), Teredo navalis (2)* and *Nototeredo norvagica (3).*

	Site	Season	Post_dep	DOS	pH	T°	Salinity	H2S	1	2
Site										
Season	-0.075									
Post_dep	-0.157	0.211								
DOS	0.412*	-0.458*	0.154							
pH	0.474**	-0.389*	0.138	0.564**						
T°	-0.062	0.979***	0.165	-0.469**	-0.495**					
Salinity	-0.087	-0.265	0.056	0.351	0.202	-0.286				
H2S	-0.544**	0.456**	0.342	-0.304	-0.34	0.412*	0.127			
L. mersinensis (1)	0.075	0.151	-0.618***	-0.302	-0.178	0.165	-0.414*	-0.201		
T. navalis (2)	0.268	-0.587***	-0.478**	0.017	-0.012	-0.538**	0.135	-0.279	0.112	
N. norvagica (3)	0.479**	0.017	-0.041	0.069	0.126	0.074	-0.306	-0.355*	0.099	0.051

Discussion

Species coverage

The World Register of Marine Species (WORMS) lists 98 accepted Teredinidae species (https://www.marinespecies.org). In Europe 9 species are established (Borges et al., 2014a; Borges & Merckelbach, 2018). The Mediterranean harbours 7 species with four also being found in other European waters (Borges et al., 2014a; Borges & Merckelbach, 2018; Tagliapietra et al., 2021). Most of these species have a wide distribution beyond Europe (Turner 1966, (https://invasions.si.edu/nemesis/species_summary/ 81862). The only exception is *Lyrodus mersinensis.* This species was described recently with a distribution limited to the Mediterranean, making it the only living endemic shipworm for the Mediterranean at this date (Borges & Merckelbach, 2018). In this study almost half of the Mediterranean and the majority of the five species of the northern Adriatic Sea were found. I identified *Lyrodus mersinensis, Teredo navalis* and *Nototeredo norvagica*.

Bankia carinata

My first hypothesis based on the findings of Borges et al. (2014a) was rejected as *Bankia carinata* was not found during the project. Similar to *Nototeredo norvagica, B. carinata* is oviparous with larvae free-living in the water for a couple of weeks (Nair & Saraswathy, 1971; Turner, 1966). *N. norvagica* established itself at two sites, therefore the reproductive strategy should not be the limiting factor for *B. carinata.* The distribution of marine organisms can be influenced by many abiotic parameters (Gogina & Zettler, 2010; Turner, 1966). Temperature, salinity and wood availability seem to be the most important for shipworms (Nair & Saraswathy, 1971; Turner, 1966). Borges et al. (2014a) described the temperature and salinity tolerances of *B. carinata* as 9-30°C and 35-39 ‰. Their environmental data was gathered from the oceanographic database Bio-ORACLE (Tyberghein et al., 2012). Our cube inside values ranged outside these tolerances with temperatures down to 8°C and the salinity dropping close to 34 ‰. The minimal temperature and salinity of the water surrounding the BORGs was identical. Borges et al. (2014a) suggested based on their data that B. carinata was stenohaline, preferring high salinities. Even though the differences were small compared to the proposed tolerances, this could be the reason limiting this species from settling at our sites. Interestingly, the records of *B. carinata* in the

north Adriatic Sea were from the Croatian coast, south of our sites in Slovenia (Borges et al., 2014a). It would be interesting to have a wider stretched search along the Slovenian and Italian coasts to see how far north they occur.

Temporal and spatial distribution

In Lera, only *Lyrodus mersinensis* and *Teredo navalis* were encountered. *Nototeredo norvagica* was never sampled at this site. In Strunjan and Institute *T. navalis, L. mersinensis* and *N.* norvagica occurred on the same wood cubes. Similar results were found for *T. navalis, N. norvagica* and *Lyrodus pedicellatus* in the Mediterranean (Charles et al., 2018). Note that in Charles et al. (2018), the shipworms were identified on morphology alone. Given the geographical position and the lack of molecular data, Charles et al. (2018) could have dealt with *L. mersinensis* instead. My assumptions of Lera and Strunjan being easier to colonise based on wood vicinity in comparison to Institute were not met. To the contrary, in Institute all three species were found with *T. navalis* occurring one summer. My third hypothesis was rejected as Lera was more inaccessible, and Institute being easier to colonise for the shipworms. The temperature and salinity inside the cubes and at the BORGs at the three sites Lera, Strunjan and Institute were all in the temperature and salinity tolerances of *L. mersinensis, T. navalis* and *N. norvagica* suggested by Borges et al. (2014a) (Borges & Merckelbach, 2018). In Charles et al. (2018), *N. norvagica* grew the largest. Although our shipworms were not measured, I observed the same pattern upon sampling. Individuals of *N. norvagica* had the biggest body size out of the three species. This makes sense as spawners have been described to grow significantly larger than brooders in the same timeframe (Macintosh et al., 2014).

- *Time of colonisation*

The late arrival of *Nototeredo norvagica* at Strunjan and Institute could be linked to its reproduction period. *N. norvagica* reproduces in late fall to early winter in colder waters (Nair, 1962; Turner, 1966). This breeding period seemed to be extended or shifted at our sites. This species was observed to release white dots, probably eggs and sperm, during sampling in early March in 2021. In summer 2021 I did not observe this behaviour. According to Turner (1966), every shipworm species has its optimum temperature for spawning. In the northern Adriatic Sea this temperature probably occurred over a longer period allowing longer

breeding/spawning. A prolonged reproduction period in warmer waters was observed in Appelqvist & Havenhand (2016). In their laboratory experiments, *Teredo navalis* spawned the sperm at 14°C and released its larvae at 16-20°C (Loosanoff & Davis, 1963). This fitted the results of Appelqvist & Havenhand (2016) in the wild, showing *T. navalis* recruiting new wood from end of June until beginning of October with the highest activity from end of July until end of September in Sweden. In the warmer northern Adriatic Sea, compared to the Swedish coast, this timeframe could be extended further. Unfortunately, there was no data on the reproduction of *Lyrodus mersinensis.* Based on our findings, it could have a similar reproduction period as *T. navalis.* Still, a delayed reproduction of *N. norvagica* should not exclude this species from the first winter sampling. It should have been able to settle on our cubes before the first sampling in February.

- *Nototeredo norvagica absent in Lera*

Nototeredo norvagica was not able to colonize Lera. There could be various reasons. Temperature, salinity and wood availability are the most important factors for the distribution of shipworms (Nair & Saraswathy, 1971; Turner, 1966). As mentioned above, the temperature and salinity did not seem to be the limiting factor. The high H_2S concentration and the low pH could play a role, but the influence of these factors has yet to be researched. It could be linked to the reproduction strategy. *N. norvagica* is an oviparous spawner, releasing small eggs and sperm resulting in free swimming larvae (Lebour, 1946; Turner, 1966). This reproductive strategy differs from the other two species. *Teredo navalis* is a short-term larviparous species that broods the young until the straight hinge veliger larvae (Johnson & Turner, 1971; Turner, 1966). For the recently described *Lyrodus mersinensis* there was no record. The genus *Lyrodus* is characterized by long term brooding (Borges et al., 2012; Turner, 1966). *Lyrodus floridanus* (Bartsch. 1922), a cryptic species of *L. pedicellatus* shakes this generalisation, as it is characterized by its short-term brooding. Still, all known *L.* sp. brood. Based on this, I assumed that *L. mersinensis* is most probably a brooder too, either short- or long term. The less developed sperm, eggs and larvae of *N. norvagica* could be more susceptible to unfavourable conditions compared to the further developed larvae of *T. navalis* and *L. mersinensis*, thus not surviving long enough to settle in Lera. To link a difference in the duration of the free-swimming period is difficult, as short-term brooders can have a similar long swimming period as oviparous

spawners (Johnson & Turner, 1971). A major factor to consider is the reproduction period. As we explored above, *N. norvagica* reproduces later than *T. navalis* and probably *L. mersinensis* (Appelqvist & Havenhand, 2016; Nair, 1962). Although this alone should not exclude this species from settling in Lera. Nair (1962) observed *N. norvagica* settling at less colonized and overgrown wood sections, seemingly avoiding competition and overgrowth by other organisms. If it was actively avoiding these parts or just being unable to settle in the more populated wood parts is not known. Interestingly Lera was the subject of the most colonisation and overgrowth by organisms, especially ascidians. By the time of settling, the cubes could have been already too overgrown leading *N. norvagica* not wanting or being able to settle. In addition, instead of being able to settle they could serve as food for the abundant filter-feeding ascidians.

- *Teredo navalis missing in summer*

Teredo navalis was found at different sites in consecutive winters but was missing in summer. This pattern of *T. navalis* at Lera, Strunjan and to some extend in Institute suggests local extinctions on our cubes and multiple colonisation events. This pattern contrasts with literature, observing *T. navalis* throughout the summer (Charles et al., 2018; Tuente et al., 2002). Something affected *T. navalis* during spring/early summer at our sites leading to its disappearance in the warmer season. It is difficult to pinpoint a reason, there are some possibilities I will briefly explore. The first is the temperature difference in spring/summer. It is unlikely to be the cause as temperature and salinity were in the tolerances of adult and pediveligers of *T. navalis* (Borges et al., 2014; Hoagland, 1986). The second one is competition between shipworms. In Charles et al. (2018) *T. navalis, Lyrodus pedicellatus* (most probably *L. mersinensis)* and *Nototeredo norvagica* were found on the same cubes, with *T. navalis* representing over 45% of individuals. Thus, competition between these species does not explain this pattern. The substrate can be left out as cause as well. In Charles et al. (2018) pine wood, same as in this study, was used as substrate. Another factor could be H_2S concentrations. There is some evidence showing high concentrations of hydrogen sulphide and copper sulphate inhibiting shipworm settlement or survival of shipworms in the area (Hartley, 1840). It would fit our pattern. In summer, we measured higher H_2S concentrations. *T. navalis* was found in summer only in Institute, the site with the lowest H_2S concentration. The spearman correlation showed a significant

difference in sulphide between the sites. But there are downsides. The presence/absence of *T. navalis* was not significantly affected from the H_2S measurements according to our data. Also *T. navalis* was the only species to be affected by this. Unfortunately, nothing is known for the H_2S tolerances of specific shipworm species. There is no direct resolution here, but it sparks the question if and how H_2S naturally produced in wood affects different shipworm species.

- *After three years*

The last sampling stay, after three years of deployment no shipworms were found anymore. For Strunjan and Institute the cubes were disintegrated or falling apart at that point. For shipworms wood is both habitat and wood. They destroy their habitat by feeding and growing until this resource ceases and the inevitably perish (Macintosh et al., 2014). This seems to be the case in Strunjan and Institute, where the wood cubes broke down and fell of the BORG at some point. Over time, the cubes consisted more and more of dead animals and so called “ghost tunnels” containing only remains, like shells similar to the descriptions in Charles et al. (2018). In Lera the wood cubes were in good shape after three years, suggesting the missing larger *Nototeredo norvagica* to play a major role in the destruction of the wood cubes.

Shipworm identification

- *Sequencing*

Molecular identification was proven to be very important in this study, as it enabled us to identify *Lyrodus mersinensis* and the morphospecies *Teredo bartschi* as *Teredo navalis* accurately. I encountered some problems on my part with shorter 18S sequences caused by our universal primers. As mentioned in the results, these missing parts at the 5’end of the 18S sequences disabled me to identify *L. mersinensis* with 18S rRNA alone. The COI sequences enabled me to identify *L. mersinensis.* Similarly, the COI sequences were important in the clear identification of the morphospecies *T. bartschi* as *T. navalis.* In the latter case, all these samples clustered with 100% pairwise similarity together for the 18S. The COI sequences clustered like the 18S. The need for a second barcode was due to evidence showing 18S sequences not distinguishing shipworm species a possibility (Treneman et al., 2018). There were no available 18S rRNA sequences for *T. bartschi* in GenBank, so this possibility could not be ruled out. We were able

to overcome this hurdle with COI, as there was a reference in GenBank. Generally, COI has with around 20% a higher pairwise distances between species than 18S with around 0.3 to 4 % in shipworms (Borges et al., 2012, 2022; Treneman et al., 2018). The high interspecific differences in COI in shipworms is comparable to gastropods, heteropods and pteropods (Radulovici et al., 2010). The absence of intraspecific difference in 18S is known from different bivalve genera, including shipworms (Borges et al., 2012; Espińeira et al., 2009; Treneman et al., 2018). The interspecific similarity for our 18S sequences was similar to other shipworm studies (Borges et al., 2012, 2022). As seen above, the 18S rRNA barcode had some drawbacks. COI has the risk of pseudogene co-amplification (Song et al., 2008). In several studies 18S and COI barcodes are used in tandem to overcome these limitations (Borges et al., 2022; J. R. Shipway et al., 2014; Treneman et al., 2018).

- *Teredo bartschi* in the northern Adriatic Sea

I identified three samples as the morphospecies *Teredo bartschi.* The 18S sequences and COI sequences disagreed, resulting in the final identification of these samples as *Teredo navalis*. This could stem from inexperience by my part, though I compared during identification my morphospecies of *T. bartschi* and *T. navalis* with pictures from (Tagliapietra et al., 2021). My morphospecies *T. bartschi* and *T. navalis,* looked like the morphological identified *T. bartschi* and *T. navalis* in their paper. In Tagliapietra et al. (2021), the species were identified solely on morphology as in other papers before (Borges et al., 2014b; Cragg et al., 2009). But in Tagliapietra et al. (2021), it is reported that samples were stored in 95% alcohol for sequencing later. Currently, no molecular data has been published. Only 2 mitochondrial genomes of *T. bartschi* are available on NCBI and none from the Atlantic or its sub seas. This molecular data would have greatly enriched the GenBank and been the first published nuclear barcode from this species. So, it opens the question why no sequences have been published to date. It opens the possibility of *T. bartschi* from the lagoon of Venice to be a phenotype of *T. navalis* instead. Although the expectations were made based on the results of Tagliapietra et al. (2021), the lack of *Teredo bartschi* at the sites rejects my second hypothesis.

- *Limitations of morphology*

The cryptic species *Lyrodus mersinensis* needed molecular identification in our study. With the rise of new shipworm species, often cryptic, morphology often does not suffice for accurate identification (Borges et al., 2022; Borges & Merckelbach, 2018; Macintosh, 2012). In the Mediterranean, *Lyrodus pedicellatus* is still often identified in recent papers (Sivrikaya, 2019; Tagliapietra et al., 2021). Here the shipworms were identified solely on morphology without mentioning cryptic species. The accurate geographical distributions for both species are therefore not comprehendible in the Mediterranean.

- *Phylogenetic trees*

After excluding a nucleotide at the position 449 in our 18S sequences the maximum likelihood and maximum parsimony trees were coherent, with one difference. *Lyrodus pedicellatus* (JF899211) differentiated itself from the other references. In Borges et al. (2012) *L. pedicellatus* (JF899211) also stood out. In their study this sample from Florida was suggested to be the cryptic species *Lyrodus floridanus* (Bartsch, 1922) instead (Borges et al., 2012). Another reference that stood out to me was *L. pedicellatus* (KU201123). This sample was collected in Mersin, Turkey. Upon a closer look, this 18S sequence had the nucleotide belonging to *Lyrodus mersinensis*. It was the only reference of *L. pedicellatus* used in this study having that nucleotide. Therefore, I suggest this sample to be *L. mersinensis* instead. An additional COI sequence would give assurance. If correct, this would be the first full length 18S sequence of *L.* mersinensis on GenBank.

The sample 6545 stood out in the 18S and COI phylogenetic trees. For both barcodes this sample was the sister taxa to *Nototeredo norvagica.* The morphology also belonged to the same species. The differences were in the 5'end for the 18S sequence, where the quality was lower. All in all, the sequence quality of this sample was at the lower end among our samples. Despite this it was identified as *N. norvagica* based on the combined results.

Conclusion

The shipworm identification came with its hurdles. It showed that morphological identification alone lacks the resolution for complete identification. With the description of cryptic species, the use of multiple molecular barcodes becomes a

necessity. The identification key of Turner 1971b, being a monumental resource, would benefit from an update: be it just including newer species to raise awareness of cryptic species or even have pictures as additional reference. The ecological results opened a lot to discuss. Temperature and salinity were not enough to explain the presence or absence of shipworm species at our sites. Different possibilities sprung up and an interesting question arose. Does hydrogen sulphide, occurring naturally in wood, significantly impact the settlement and survival of shipworm species? The answer to this question awaits a future investigation.

Appendix

Zusammenfassung

Schiffsbohrwürmer sind eine hoch angepasste Gruppe von Bivalven, wovon die meisten Holz zersetzen. Sie entfliehen den meisten Erhebungen. Durch diese Eigenschaften können sie große Schäden verursachen, bevor man sie bemerkt. Für meine Masterarbeit habe ich diese Tiere im nordadriatischen Meer bestimmt. Entlang der slowenischen Küste wurden an drei Standorten (Lera, Strunjan, Institute) von Sommer 2019 bis Sommer 2022, Holzwürfel versenkt. Proben wurden zweimal jährlich erhoben. Die Schiffsbohrwürmer wurden anhand von Morphologie und Sanger Sequenzierung bestimmt. Dafür wurde die nukleare 18S rRNA verwendet. Für einige Proben wurden zusätzlich COI-Sequenzen von Gäelle Berte generiert. Die morphologische Identifikation ergab vier Arten. Die endgültige Bestimmung, mit Rücksichtnahme auf die Sequenzen ergab jedoch die drei Arten *Nototeredo norvagica, Teredo navalis* und die kryptische Art *Lyrodus mersinensis.* Die Morphospezies *Teredo bartschi* erwies sich am Ende als *T. navalis.* Dieses Phänomen könnte an mangelnder Erfahrung meinerseits liegen, jedoch wirft es auch Fragen auf für die in der Gegend exklusiv morphologisch bestimmten *T. bartschi.* Die Bestimmung der Schiffsbohrwürmer kam mit einigen Herausforderungen, hat aber gezeigt wie wichtig DNA-Barcoding ist. *Bankia carinata*, bekannt in dem nordadriatischen Meer wurde nicht angetroffen. In Strunjan und Institute wurden alle drei bestimmten Arten gefunden. In Lera waren es nur *L. mersinensis* und *T. navalis.* Die Präsenz der Arten an den verschiedenen Standorten konnte nicht durch Temperatur, Salinität und Holz in der Nähe erklärt werden. Unterschiede in der sessilen, filtrierenden Tiergemeinschaften am Holz und Unterschiede im natürlich produzierte und austretenden Schwefelwasserstoff während der Holzzersetzung, könnte die Präsenz der Schiffsbohrwürmer beeinflussen. Diese Fragen benötigen allerdings zukünftige Untersuchungen.

References

ABP Biosciences (last accessed 17.05.2023). https://www.abpbio.com

Altschul, S. F., Gish, W., Miller, W., Myers, E. W., & Lipman, D. (1990). Basic local alignment search tool. *Journal of Molecular Biology*, 215(3), 403–410. https://doi.org/10.1016/S0022-2836(05)80360-2

Appelqvist, C., & Havenhand, J. N. (2016). A phenological shift in the time of recruitment of the shipworm, Teredo navalis L ., mirrors marine climate change. *Ecology and Evolution,* 6(12), 3862–3870. https://doi.org/10.1002/ece3.2126

Archie, J., Day, W. H. E., Maddison, W., Meacham, C., Rohlf, F. J., Swofford, D., & Felsenstein, J. (1986). The Newick tree format. http://evolution.genetics.washington.edu/phylip/newicktree.html

Borges, L. M. S., & Merckelbach, L. M. (2018). Lyrodus mersinensis sp. nov. (Bivalvia: Teredinidae) another cryptic species in the Lyrodus pedicellatus (Quatrefages, 1849) complex. *Zootaxa*, 4442(3), 441–457. https://doi.org/10.11646/zootaxa.4442.3.6

Borges, L. M. S., Merckelbach, L. M., Sampaio, Í., & Cragg, S. M. (2014a). Diversity, environmental requirements, and biogeography of bivalve wood-borers (Teredinidae) in European coastal waters. *Frontiers in Zoology*, 11(13). https://doi.org/https://doi.org/10.1186/1742-9994-11-13

Borges, L. M. S., Sivrikaya, H., & Cragg, S. M. (2014b). First records of the warm water shipworm Teredo bartschi Clapp, 1923 (Bivalvia, teredinidae) in Mersin, southern Turkey and in Olhão, Portugal. *BioInvasions Records*, 3(1), 25–28. https://doi.org/10.3391/bir.2014.3.1.04

Borges, L. M. S., Sivrikaya, H., le Roux, A., Shipway, J. R., Cragg, S. M., & Costa, F. O. (2012). Investigating the taxonomy and systematics of marine wood borers (Bivalvia: Teredinidae) combining evidence from morphology, DNA barcodes and nuclear locus sequences. *Invertebrate Systematics*, 26, 572–582. https://doi.org/http://dx.doi.org/10.1071/IS12028

Borges, L. M. S., Treneman, N. C., Haga, T., Shipway, J. R., Raupach, M. J., Altermark, B., & Carlton, J. T. (2022). Out of taxonomic crypsis: A new trans-arctic cryptic species pair corroborated by phylogenetics and molecular evidence. *Molecular Phylogenetics and Evolution*, 166. https://doi.org/10.1016/j.ympev.2021.107312

Borojevic, K., Steiner, W. E., Gerisch, R., Zazzaro, C., & Ward, C. (2010). Pests in an ancient Egyptian harbor. *Journal of Archaeological Science*, 37(10), 2449–2458. https://doi.org/10.1016/j.jas.2010.04.013

Charif, D., Clerc, O., Frank, C., Lobry, J. R., Necsulea, A., Palmeira, L., Penel, S., & Perrière, G. (2021). Biological Sequences Retrieval and Analysis. http://seqinr.r-forge.r-project.org/

Charles, F., Coston-Guarini, J., Guarini, J.-M., & Lantoine, F. (2018). It's what's inside that counts: computer-aided tomography for evaluating the rate and extent of wood consumption by shipworms. *Journal of Wood Science*, 64, 427–435. https://doi.org/10.1007/s10086-018-1716-x

Combosch, D. J., Collins, T. M., Glover, E. A., Graf, D. L., Harper, E. M., Healy, J. M., Kawauchi, G. Y., Lemer, S., McIntyre, E., Strong, E. E., Taylor, J. D., Zardus, J. D., Mikkelsen, P. M., Giribet, G., & Bieler, R. (2017). A family-level Tree of Life for bivalves based on a Sanger-sequencing approach. *Molecular Phylogenetics and Evolution*, 107, 191–208. https://doi.org/10.1016/j.ympev.2016.11.003

Connor, R. M., Fung, J. M., Sharp, K. H., Benner, J. S., McClung, C., Cushing, S., Lamkin, E. R.,

Fomenkov, A. I., Henrissat, B., Londer, Y. Y., Scholz, M. B., Posfai, J., Malfatti, S., Tringe, S. G., Woyke, T., Malmstrom, R. R., Coleman-Derr, D., Altamia, M. A., Dedrick, S., … Distel, D. L. (2014). Gill bacteria enable a novel digestive strategy in a wood-feeding mollusk. *Proceedings of the National Academy of Sciences*, 111(47), 5096–5104. https://doi.org/10.1073/pnas.1413110111

Cornish-Bowden, A. (1985). Nomenclature for incompletely specified bases in nucleic acid sequences: rcommendations 1984. *Nucleic Acids Research*, 13(9), 3021–3030. https://doi.org/10.1093/nar/13.9.3021

Cragg, S. M., Jumel, M. C., Al-Horani, F. A., & Hendy, I. W. (2009). The life history characteristics of the wood-boring bivalve Teredo bartschi are suited to the elevated salinity, oligotrophic circulation in the Gulf of Aqaba, Red Sea. *Journal of Experimental Marine Biology and Ecology*, 375(1–2), 99–105. https://doi.org/10.1016/j.jembe.2009.05.014

Distel, D. L. (2003). The Biology of Marine Wood Boring Bivalves and Their Bacterial Endosymbionts. In B. Goodell, D. D. Nicholas, & T. P. Schultz (Eds.), *Wood Deterioration and Preservation,* 845, 253–271 https://doi.org/10.1021/bk-2003-0845.ch014

Distel, D. L., Altamia, M. A., Lin, Z., Shipway, J. R., Han, A., Forteza, I., Antemano, R., Gwen, M., Limbaco, J. P., Tebo, A. G., Dechavez, R., Albano, J., Rosenberg, G., Concepcion, G. P., Schmidt, E. W., & Haygood, M. G. (2017). Discovery of chemoautotrophic symbiosis in the giant shipworm Kuphus polythalamia (Bivalvia: Teredinidae) extends wooden-steps theory. *Proceedings of the National Academy of Sciences*, 114(18), 3652–3658. https://doi.org/10.1073/pnas.1620470114

Distel, D. L., Amin, M., Burgoyne, A., Linton, E., Mamangkey, G., Morrill, W., Nove, J., Wood, N., & Yang, J. (2011). Molecular phylogeny of Pholadoidea Lamarck, 1809 supports a single origin for xylotrophy (wood feeding) and xylotrophic bacterial endosymbiosis in Bivalvia. *Molecular Phylogenetics and Evolution*, 61(2), 245–254. https://doi.org/10.1016/j.ympev.2011.05.019

Edgar, R. C. (2004). MUSCLE: Multiple sequence alignment with high accuracy and high throughput. *Nucleic Acids Research*, 32(5), 1792–1797. https://doi.org/10.1093/nar/gkh340

Elwood, H. J., Olsen, G. J., & Sogin, M. L. (1985). The small-subunit ribosomal RNA gene sequences from the hypotrichous ciliates Oxytricha nova and Stylonychia pustulata. *Molecular Biology and Evolution*, 2(5), 399–410. https://doi.org/10.1093/oxfordjournals.molbev.a040362

Espińeira, M., González-Lavín, N., Vieites M., J., & Santaclara, F. J. (2009). Development of a Method for the Genetic Identification of Commercial Bivalve Species Based on Mitochondrial 18S rRNA Sequences. *Journal of Agricultural and Food Chemistry*, 57(2), 495–502. https://doi.org/10.1021/jf802787d

Felsenstein, J. (2013). PHYLIP (Phylogeny Inference Package) version 3.696. distributed by the author. Seattle: Department of Genome Sciences, University of Washington.

Folmer, O., Black, M., Hoeh, W., Lutz, R., & Vrijenhoek, R. (1994). DNA primers for amplification of mitochondrial cytochrome c oxidase subunit I from diverse metazoan invertebrates. *Molecular Marine Biology and Biotechnology*, 3(5), 294–299. https://doi.org/10.3390/ani13152505.

Fuller, S. C., Hu Y.P., Lutz, R. A., & Castagna, M. (1989). Shell and pallet morphology in early developmental stages of Teredo navalis Linné (Bivalvia, Teredinidae). *Nautilus*, 103, 24–35. https://www.biodiversitylibrary.org/item/34236#page/42/mode/1up

Giribet, G., & Wheeler, W. (2005). On bivalve phylogeny: a high-level analysis of the Bivalvia (Mollusca) based on combined morphology and DNA sequence data. *Invertebrate Biology*,

121(4), 271–324. https://doi.org/https://doi.org/10.1111/j.1744-7410.2002.tb00132.x

Gogina, M., & Zettler, M. L. (2010). Diversity and distribution of benthic macrofauna in the Baltic Sea: Data inventory and its use for species distribution modelling and prediction. *Journal of Sea Research*, 64(3), 313–321. https://doi.org/10.1016/j.seares.2010.04.005

Gouy, M., Guindon, S., & Gascuel, O. (2010). SeaView version 4: A multiplatform graphical user interface for sequence alignment and phylogenetic tree building. *Molecular Biology and Evolution*, 27(2), 221–224. https://doi.org/10.1093/molbev/msp259

Guindon, S., Dufayard, J. F., Lefort, V., Anisimova, M., Hordijk, W., & Gascuel, O. (2010). New Algorithms and Methods to Estimate Maximum-Likelihood Phylogenies: Assessing the Performance of PhyML 3.0. *Systematic Biology*, 59(3), 307–321. https://doi.org/10.1093/sysbio/syq010

Harrel Jr., F. E. (2023). Hmisc: Harrell Miscellaneous. R package version 5.0-1. https://cran.rproject.org/package=Hmisc

Hartley, J. B. (1840). On the Effects of the Worm on Kyanized Timber Exposed to the Action of Sea Water, and on the Use of Greenheart Timber from Demerara, in the Same Situations. *Minutes of the Proceedings of the Institution of Civil Engineers*, 1(1840), 84–85. https://doi.org/10.1680/imotp.1840.24926

Hoagland, K. E. (1986). Effects of Temperature, Salinity, and Substratum on Larvae of the Shipworms Teredo bartschi Clapp and Teredo navalis Linnaeus (Bivalvia, Teredinidae). *American Malacological Bulletin*, 4(1), 89-99. https://www.biodiversitylibrary.org/partpdf/143169

Johnson, A. C., & Turner, R. D. (1971). Biology of marine wood-boring molluscs. In E. B. G. Jones & S. K. Eltringham (Eds.), *Marine Borers, Fungi, and Fouling Organisms of Wood* (pp. 259–301)

Kamburska, L., Lauceri, R., Beltrami, M., Boggero, A., Cardeccia, A., Guarneri, I., Manca, M., & Riccardi, N. (2013). Establishment of Corbicula fluminea (O.F. Müller, 1774) in Lake Maggiore: a spatial approach to trace the invasion dynamics. *BioInvasions Records*, 2(2), 105–117. https://doi.org/10.3391/bir.2013.2.2.03

Kos, M. (2021). Port traffic of vessels in 2020 lower than in 2019. https://www.stat.si/StatWeb/en/news/Index/9708

Lebour, M. (1946). The Species of Teredo from Plymouth Waters. *Journal of the Marine Biological Association of the United Kingdom*, 26(3), 381–389. https://doi.org/10.1017/S0025315400012200

Lee, S. Y., Mohamed, R., & Lamasudin, D. U. (2019). Morphology and molecular phylogenetic placement of a coastal shipworm (Bactronophorus thoracites (Gould, 1862), Teredinidae) from Peninsular. *Regional Studies in Marine Science*, 29. https://doi.org/10.1016/j.rsma.2019.100694

Li, Y., Altamia, M. A., Shipway, J. R., Brugler, M. R., Bernardino, A. F., de Brito, T. L., Lin, Z., da Silva Oliveira, F. A., Sumida, P., Smith, C. R., Trindade-Silva, A., Halanych, K. M., & Distel, D. L. (2022). Contrasting Modes of Mitochondrial Genome Evolution in Sister Taxa of Wood-Eating Marine Bivalves (Teredinidae and Xylophagaidae). *Genome Biology and Evolution*, 14(6). https://doi.org/10.1093/gbe/evac089

Linnaeus, C. (1758). Systema Naturae per regna tria naturae, secundum classes, ordines, genera, species, cum characteribus, differentiis, synonymis, locis (10th ed., Vol. 1). https://www.biodiversitylibrary.org/bibliography/542

Loosanoff, V. L., & Davis, H. C. (1963). Rearing Of Bivalve Mollusks. *Advances in Marine Biology*, 1, 1–136. https://doi.org/10.1016/S0065-2881(08)60257-6

Macintosh, H. (2012). Lyrodus turnerae, a new teredinid from eastern Australia and the Coral Sea (Bivalvia: Teredinidae). *Molluscan Research*, 32(1), 36–42.

Macintosh, H., de Nys, R., & Whalan, S. (2014). Contrasting life histories in shipworms: Growth, reproductive development and fecundity. *Journal of Experimental Marine Biology and Ecology*, 459, 80–86. https://doi.org/10.1016/j.jembe.2014.05.015

Medlin, L., Elwood, H. J., Stickel, S., & Sogin, M. L. (1988). The characterization of enzymatically amplified eukaryotic 16S-like rRNA-coding regions. *Gene*, 71(2), 491–499. https://doi.org/10.1016/0378-1119(88)90066-2

Microsoft Corporation. (2018). Microsoft Excel. https://office.microsoft.com/excel

Moranta, J., Quetglas, A., Massuti, E., Guijarro, B., Ordines, F., & Maria, V. (2008). Research Trends on Dermersal Fisheries Oceanography in the Mediterranean. In C. V. Rades & E. B. Tilesman (Eds.), Advances in Environmental Research (1st ed., pp. 1–57). *Nova Publishers*. https://books.google.lu/books?hl=en&lr=&id=BAsy2dy75PMC&oi=fnd&pg=PA1&dq=Morantta,+Joan%3B+Quetglas,+Antoni%3B+Massutí,+Enric%3B+Guijarro,+Beatriz%3B+Ordines,+Francesc%3B+Valls,+María+(2008).+%22Research+trends+on+demersal+fisheries+oceanography+in+the+Med

Nair, N. B. (1962). Ecology of marine fouling and wood-boring organisms of Western Norway. *Sarsia*, 8(1), 1–88. https://doi.org/10.1080/00364827.1962.10410269

Nair, N. B., & Saraswathy, M. (1971). The biology of wood-boring teredinid molluscs. *Advances in Marine Biology*, 9, 335–509. https://doi.org/10.1016/S0065-2881(08)60345-4

Smithsonian Environmental Research Center's National Estuarine and Marine Exotic Species Information System (NEMESIS) (last accessed 19.05.2022). https://invasions.si.edu/nemesis/species_summary/81862

Nelson, D. L. (2018). Shipworms and the Making of the American Coastline. *ProQuest Dissertations & Theses Global*, Order No.(2055753829). https://www.proquest.com/dissertations-theses/shipworms-making-american-coastline/docview/2055753829/se-2?accountid=162526

Ooms, J. (2023). writexl: Export Data Frames to Excel "xlsx" Format. R package version 1.4.2. (1.4.2).

Paalvast, P., & Velde, G. Van Der. (2011). New threats of an old enemy: The distribution of the shipworm Teredo navalis L . (Bivalvia : Teredinidae) related to climate change in the Port of Rotterdam area , the Netherlands. *Marine Pollution Bulletin*, 62(8), 1822–1829. https://doi.org/10.1016/j.marpolbul.2011.05.009

Paradis, E., & Schliep, K. (2019). ape 5.0: an environment for modern phylogenetics and evolutionary analyses in R. *Bioinformatics*, 35(3), 526–528. https://doi.org/10.1093/bioinformatics/bty633

Poulain, P.-M., Kourafalou, V. H., & Cushman-Roisin, B. (2001). Northern Adriatic Sea. In B. Cushman-Roisin, M. Gačić, P. Poulain, & A. Artegiani (Eds.), Physical Oceanography of the Adriatic Sea (pp. 143–165). https://doi.org/10.1007/978-94-015-9819-4

R Core Team. (2013). R: A language and environment for statistical computing. R Foundation for Statistical Computing. http://www.r-project.org/

Radulovici, A. E., Archambault, P., & Dufresne, F. (2010). DNA Barcodes for Marine Biodiversity: Moving Fast Forward? *Diversity*, 2(3), 450–472. https://doi.org/10.3390/d2040450

Ratnasingham, S., & Hebert, P. D. N. (2007). BOLD: The Barcode of Life Data System. *Molecular Ecology Notes*, 7(3), 355–364. https://doi.org/10.1111/j.1471-8286.2006.01678

Robin, N., Velásquez, M., Boura, A., Garcia, G., Jauvion, C., Boiteau, J., Gomez, B., Daviero-Gomez, V., & Valentin, X. (2018). The oldest shipworms (Bivalvia, Pholadoidea, Teredinidae) preserved with soft parts (western France): insights into the fossil record and evolution of Pholadoidea. *Palaeontology*, 61(6), 905–918. https://doi.org/10.1111/pala.12376

Sayers, E. W., Bolton E. E., Brister, J. R., Canese, K., Chan, J., Comeau, D. C., Connor, R., Funk, K., Kelly, C., Kim, S., Madej, T., Marchler-Bauer, A., Lanczycki, C., Lathrop, S., Lu, Z., Thibaud-Nissen, F., Murphy, T., Phan, L., … Sherry, S. T. (2022). Database resources of the National Center for Biotechnology Information. *Nucleid Acids Research,* 50 (D1): D20-D26. (last accessed 19.06.2023) https://doi.org/10.1093/nar/gkab1112

Sellius, G. (1733). Historia Naturalis Teredinis Seu Xylophagi Marini Tubulo-Conchoidis Speciatim Belgici, Trajecti ad Rhenum. https://books.googleusercontent.com/books/content?req=AKW5QafsEOk71QRiLExYXQUISIRXQgJWsQv_6BGGrSAdfdSKSbrIx-bpg88nUXp4JZKd-OrWOOv4fVwI3dAHpHAZ0l0h0ng1fgxwVKJXSLev981GgTXRoNtdBS_1vFGGuGQNZZ5r1VlS5lYN1jn6y6zpYBHziNTFjD3f5h_qiHvfHj-0ip_weHSfAXc60RZn8_5wgmPwX

Shipway, J. R., Borges, L. M. S., Müller, J., & Cragg, S. M. (2014). The broadcast spawning Caribbean shipworm, Teredothyra dominicensis (Bivalvia, Teredinidae), has invaded and become established in the eastern Mediterranean Sea. *Biological Invasions*, 16, 2037–2048. https://doi.org/10.1007/s10530-014-0646-9

Shipway, J. R., O'Connor, R., Stein, D., Cragg, S. M., Korshunova, T., Martynov, A., Haga, T., & Distel, D. L. (2016). Zachsia zenkewitschi (Teredinidae), a Rare and Unusual Seagrass Boring Bivalve Revisited and Redescribed. *PLOS ONE*, 11(5), e0155269. https://doi.org/10.1371/journal.pone.0155269

Shipway, J. Reuben, Altamia, M. A., Rosenberg, G., Concepcion, G. P., Haygood, M. G., & Distel, D. L. (2019). A rock-boring and rock-ingesting freshwater bivalve (shipworm) from the Philippines. *Proceedings of the Royal Society B*, 286(1905), 20190434. https://doi.org/10.1098/rspb.2019.0434

Sivrikaya, H. (2019). Investigations on Wood Destroying Marine Borers in the Turkish coastal Waters. *Wood Industry and Engineering*, 1(1), 33–39. https://www.researchgate.net/publication/338901782%0AINVESTIGATIONS

Song, H., Buhay, J. E., Whiting, M. F., & Crandall, K. A. (2008). Many species in one: DNA barcoding overestimates the number of species when nuclear mitochondrial pseudogenes are coamplified. *Proceedings of the National Academy of Sciences of the United States of America*, 105(36), 13486–13491. https://doi.org/10.1073/pnas.0803076105

Steinmayer, A. G., & Turfa, J. M. (1996). Effects of shipworm on the performance of ancient Mediterranean warships. *International Journal of Nautical Archaeology*, 25(2), 104–121. https://doi.org/10.1006/ijna.1996.0013

Sundberg, A. (2015). Molluscan Explosion: The Dutch Shipworm Epidemic of the 1730s. *Environment & Society Portal, Arcadia*, no. 14. https://doi.org/10.5282/rcc/7307

Tagliapietra, D., Guarneri, I., Keppel, E., & Sigovini, M. (2021). After a century in the Mediterranean, the warm-water shipworm Teredo bartschi invades the Lagoon of Venice

(Italy), overwintering a few degrees above zero. *Biological Invasions*, 23, 1595–1618. https://doi.org/10.1007/s10530-021-02461-3

Tamura, K., Stecher, G., & Kumar, S. (2021). MEGA11: Molecular Evolutionary Genetics Analysis Version 11. *Molecular Biology and Evolution*, 38(7), 3022–3027. https://doi.org/10.1093/molbev/msab120

Taylor, J. D., Williams, S. T., Glover, E. A., & Dyal, P. (2007). A molecular phylogeny of heterodont bivalves (Mollusca: Bivalvia: Heterodonta): new analyses of 18S and 28S rRNA genes. *Zoologica Scripta*, 36(6), 587–606. https://doi.org/10.1111/j.1463-6409.2007.00299.x

Treneman, N., Borges, L., Shipway, R., Raupach, M., Altermark, B., & Carlton, J. (2018). A molecular phylogeny of wood-borers (Teredinidae) from Japanese Tsunami Marine Debris. *Aquatic Invasions*, 13(1), 101–112. https://doi.org/10.3391/ai.2018.13.1.08

Tuente, U., Piepenburg, D., & Spindler, M. (2002). Occurrence and settlement of the common shipworm Teredo navalis (Bivalvia: Teredinidae) in Bremerhaven harbours, northern Germany. *Helgoland Marine Research*, 56, 87–94. https://doi.org/10.1007/s10152-002-0101-7

Turner, R. D. (1966). A survey and illustrated catalogue of the Teredinidae: (Mollusca: Bivalvia). *Museum of Comparative Zoology Harvard University*. https://doi.org/https://doi.org/10.5962/bhl.title.67017

Turner, R. D. (1971a). Australian Shipworms. *Australian Natural History*, 17(4), 139–145.

Turner, R. D. (1971b). Identification of marine wood boring molluscs. In E. B. G. Jones & S. K. Eltringham (Eds.), Marine Borers, Fungi, and Fouling Organisms of Wood (pp. 17–64).

Tyberghein, L., Verbruggen, H., Pauly, K., Troupin, C., Mineur, F., & De Clerck, O. (2012). Bio-ORACLE: a global environmental dataset for marine species distribution modelling. *Global Ecology and Biogeography*, 21(2), 272–281. https://doi.org/10.1111/j.1466-8238.2011.00656.x

van der Laken, P. (2020). paulvanderlaken.com. (last accessed 19.05.2023) https://paulvanderlaken.com/2020/07/28/publication-ready-correlation-matrix-significance-r/

Velásquez, M. & Shipway, J. R. (2018). A new genus and species of deep-sea wood-boring shipworm (Bivalvia: Teredinidae) Nivanteredo coronata n. sp. from the Southwest Pacific. *Marine Biology Research*, 14(8), 806-815. https://doi.org/10.1080/17451000.2018.1544421

Weigelt, R., Lippert, H., Borges, L. M. S., Appelqvist, C., Karsten, U., & Bastrop, R. (2016). First time DNA barcoding of the common shipworm Teredo navalis Linnaeus 1758 (Mollusca: Bivalvia: Teredinidae): Molecular-taxonomic investigation and identification of a widespread wood-borer. *Journal of Experimental Marine Biology and Ecology*, 475, 154–162. https://doi.org/10.1016/j.jembe.2015.11.008

Weigelt, R., Lippert, H., Karsten, U., & Bastrop, R. (2017). Genetic Population Structure and Demographic History of the Widespread Common Shipworm Teredo navalis Linnaeus 1758 (Mollusca: Bivalvia: Teredinidae) in European Waters Inferred from Mitochondrial COI Sequence Data. *Frontiers in Marine Science*, 4. https://doi.org/10.3389/fmars.2017.00196

Wickham, H, Averick, M., Bryan, J., Chang, W., McGowan, L. D., François, R., Grolemund, G., Hayes, A., Henry, L., Hester, J., Kuhn, M., Pedersen, T. L., Miller, E., Bache, S. M., Müller, K., Ooms, J., Robinson, D., Seidel, D. P., Spinu, V., … Yutani, H. (2019). Welcome to the tidyverse. *Journal of Open Source Software*, 4(43), 1686. https://doi.org/10.21105/joss.01686

Wickham, Hadley, & Bryan, J. (2022). readxl: Read Excel Files. R package version 1.4.1. 5. https://cran.r-project.org/package=readxl

Wickham, Hadley, Chang, W., Henry, L., Pedersen, T. L., Takahashi, K., Wilke, C., Woo, K., Yutani, H., & Dunnington, D. (2016). ggplot2: Elegant Graphics for Data Analysis. (3.4.0). *Springer-Verlag*. https://ggplot2.tidyverse.org

World Register of Marine Species (WoRMS). (last accessed 11.05.2023). https://www.marinespecies.org